ISTANBUL TECHNICAL UNIVERSITY ★ GRADUATE SCHOOL OF SCIENCE ENGINEERING AND TECHNOLOGY

CHARACTERISTICS OF COLD SPRAYED TITANIUM BASED COATINGS

M.Sc. THESIS

Ahmet Hilmi PAKSOY

Department of Metallurgical and Materials Engineering

Materials Engineering Programme

AUGUST 2017

ISTANBUL TECHNICAL UNIVERSITY ★ GRADUATE SCHOOL OF SCIENCE ENGINEERING AND TECHNOLOGY

CHARACTERISTICS OF COLD SPRAYED TITANIUM BASED COATINGS

M.Sc. THESIS

Ahmet Hilmi PAKSOY
(506141430)

Department of Metallurgical and Materials Engineering

Materials Engineering Programme

Thesis Advisor: Prof. Dr. Murat BAYDOĞAN
Thesis Co-Advisor: Assoc. Prof. Dr. Erdem ATAR

AUGUST 2017

ISTANBUL TEKNİK ÜNİVERSİTESİ ★ FEN BİLİMLERİ ENSTİTÜSÜ

SOĞUK GAZ DİNAMİK PÜSKÜRTME YÖNTEMİYLE ÜRETİLMİŞ TİTANYUM ESASLI KAPLAMALARIN KARAKTERİSTİĞİ

YÜKSEK LİSANS TEZİ

Ahmet Hilmi PAKSOY
(506141430)

Metalurji ve Malzeme Mühendisliği Ana Bilim Dalı

Malzeme Mühendisliği Programı

Tez Danışmanı: Prof. Dr. Murat BAYDOĞAN
Eş Danışman: Doç. Dr. Erdem ATAR

AĞUSTOS 2017

Ahmet Hilmi Paksoy, a M.Sc. student of ITU Graduate School of Science Engineering and Technology student ID 506141430, successfully defended the thesis/dissertation entitled "CHARACTERISTICS OF COLD SPRAYED TITANIUM BASED COATINGS", which he prepared after fulfilling the requirements specified in the associated legislations, before the jury whose signatures are below.

Thesis Advisor :	**Prof. Dr. Murat BAYDOĞAN** ISTANBUL Technical University	....
Co-advisor :	**Doç.Dr. Erdem ATAR** Gebze Technical University	....
Jury Members :	**Prof. Dr. Hüseyin ÇİMENOĞLU** ISTANBUL Technical University	....
	Prof. Dr. Sakin Zeytin Sakarya University	....
	Yrd. Doç. Dr. Cevat Fahir ARISOY ISTANBUL Technical University	....

Date of Submission : 1 August 2017
Date of Defense : 14 August 2017

To my family,

FOREWORD

I would like to thanks to my thesis advisors Prof. Dr. Murat BAYDOĞAN and Assoc. Prof. Dr. Erdem ATAR for their guidance, support and motivation.

I would also like to thanks to Prof. Dr. Hüseyin ÇİMENOĞLU for his guidance and supports that they displayed for my graduate education.

I would like to express my thanks to all members of Mechanical Metallurgy Group especially to M.Sc. Onur TAZEGÜL, M.Sc. Doğukan ÇETİNER and M.Sc. Faiz MUHAFFEL for their asistance in my laboratory studies and to Specialist Ahmet NAZIM from Gebze Technical University for his helps to complete the scanning electron microscopy studies.

I want to express my thanks to The Scientific and Technological Research Council of Turkey (TUBITAK, project number: 214M246) and Istanbul Technical University for their financial support.

Last but not least, I would like to express my deepest gratitude to my family and Esma YILMAZ for their support and understanding during my master study.

August 2017

Ahmet Hilmi Paksoy
(Mechanical Engineer)

TABLE OF CONTENTS

Page

ABBREVIATIONS

ASTM : American Society for Testing and Materials
SEM : Scanning Electron Microscope
OM : Optical Microscope
XRD : X-Ray Diffaction
EDX : Energy Dispersive X-Ray Spectroscopy
At. % : Atomic percentege

SYMBOLS

ϴ	**:** XRD diffaction angle
µ	**:** Friction coefficient

LIST OF TABLES

Page

LIST OF FIGURES

Page

CHARACTERISTIC OF COLD SPRAYED TITANIUM BASED COATINGS

SUMMARY

Metallic bio materials are the most common bio material group among the synthetic biomedical applications. This material group differs from the other bio materials owing to high dynamic and static strength, enough resistance to corrosion, wear and fatigue. Moreover, cobalt-chromium based alloys are one of the most favorable metallic bio materials with titanium alloys and stainless steels due to well combination of high strength, corrosion resistance and formability. Nevertheless, localized corrosion, ion releasing from the worn surfaces to the human body and other undesirable situations may lead to early failure and limit their service life to 10-12 years. Abrasion in human body is induced ion releasing and when the amount of the released ions reach to the specific level, harmful effects can be generated. Another disadvantage of these material group is poor osteointegration properties and low biocompatibility. Biocompatibility is crucial biologic property for the biomaterials because, it combines almost all the biologic properties such as bioactivity and biodegradability. Higher service life with sustainable superior properties enable the comfort patient and not necessitate painful reimplantation operations. In order to overcome the disadvantages of cobalt-chromium alloys without sacrificing its superior properties, surface modification techniques are attractive research of topic in recent years. In this master thesis study, I preferred to modify the surface of cobalt-chromium alloy with deposition of titanium based feedstock by cold gas dynamic spray process. Additionally, improvement on bioactive property aimed by the formation of titanium oxide layer on the outermost surface via the application of thermal oxidation process.

Titanium was chosen for based material because of its high biocompatibility. Although, natural oxidation of titanium provides good bioactivity and higher corrosion resistance, this oxide layer has low mechanical properties and cannot preserve the stability against to any wear condition. Hence, in the literature lots of study focused on the development of more stable oxide layers on the surface of titanium and titanium alloys. Both depositional and diffusional surface modification techniques such as micro arc oxidation and thermal oxidation etc. are used for developing titanium oxide on the surfaces. It is known from the binary phase diagram of titanium and oxygen, oxidation reaction starts at temperatures above 300^{o}C. Specific to thermal oxidation, increasing process temperature enables the formation of more stable oxide layer and thicker oxygen diffusion zone beneath it. Additionally, hardness of oxygen diffusion zone gradually decrease respect to the depth and this situation allows smooth transition from main material to brittle oxide layer and increase the wear resistance. All these advantages highlight the thermal oxidation compare to the other oxidation techniques.

Cold gas dynamic spray (CGDS) process was preferred because of simplicity and high efficiency. Possibility to form coating without any chemical reaction and/or melting, render CGDS one of the most sufficient technique among the other thermal spray techniques especially for surface modification of heat sensitive metals with high affinity to oxygen such as titanium. Moreover, extreme kinetic energies of particles

generates high impact and plastic deformation during process. Hence, it is possible to produce coating harder that substrate material.

As a part of research project (TUBITAK Project No: 214M246), in this master thesis study effect of additives on structural feature, mechanical and biological properties of titanium based coatings were investigated with the aim of improving surface properties of cobalt-chromium alloy. In that respect, feedstock containing titanium, aluminum, copper, zinc and iron oxide (in magnetite form) were prepared at different ratios and deposited on to ASTM F75 biomedical grade cobalt-chromium alloy by cold gas dynamic spray process. Then, cold sprayed substrates were thermally oxidized at 600^{o}C for 60 hour in order to obtain stable bioactive titanium based oxide layer on the outermost surface with different biological behaviors respect to compositions.

Characterization of coating were executed under the title of three different group; structural characterization, mechanical properties and biological tests. Structural surveys made by X-Ray diffraction analysis, optical and scanning electron microscope observations including area and line scan energy dispersive X-Ray spectroscopy. Additionally, roughening effect of thermal oxidation was investigated. In order to obtain mechanical properties; hardness measurements from cross section and surface, tribological test against to alumina ball in dry, serum and SBF (at 36.5 ^{o}C) testing environment were performed. In the last part of the study, biological test were done to determine effect of additives on bioactivity.

In the early stage of the study, ASTM F75 grade cobalt chromium alloy was deposited by six different feedstock composition. These feedstock consist of 92 wt.% Ti – 5 wt.% Cu – 3wt.% Fe_3O_4, 94 wt.% Ti – 3 wt.% Cu – 3wt.% Fe_3O_4, 95.5 wt.% Ti – 1.5 wt.% Cu – 3wt.% Fe_3O_4 , 87 wt.% Ti- 8 wt.% Al – 5 wt. % Zn, 89 wt. %Ti – 8 wt.%Al – 3 wt.% Fe_3O_4, 84 wt. %Ti – 8 wt.%Al – 3 wt.% Fe_3O_4 - 5 wt.% Zn. Aluminum was used to deposite titanium succesfully which has low deformation capability, without sacrificing bioactive property. While, copper and zinc were added to feedstock as an antibacterial agent, iron oxide (in magnetite form) was added to improve bioactivity and enlarge the application area of coating such as magnetic resonance imaging contrast agent, targeted drug delivery due to magnetic behavior. After deposition of feedstock, coatings thermally oxidized at 600 ^{o}C for 60 hour in normal atmospheric conditions.

Characterization of the coatings started with cross sectional optical microscope investigations of Cu containing coatings. Copper content in the feedstock were decreased to avoid from possible formation of toxic copper oxide phases during thermal oxidation. Initial obtained results showed that, when the copper content decrease, coatings show high porosities and discontinuities on the interface of coating and substrate. Hence, 5 wt.% Cu containing feedstock was chosen with the composition 92 wt.% Ti – 5 wt.% Cu – 3wt.% Fe_3O_4 for further structural investigations, determination of mechanical properties and biological tests.

Scanning electron microscope examinations showed that all the coatings before thermal oxidation exhibit almost none porosity. On the other hand, porosity level increased to rational values after thermal oxidation while around 2 µm thick oxide layer formed on the outermost surface. Moreover, area and line scan energy dispersive X-Ray spectroscopies showed well distribution of additives in coating and oxide layer. Once more for the all coating, determination of oxygen containing phases even in close regions to substrate shows well diffusion of oxygen during thermal oxidation. More specifically, in the observation of Cu containing coating, titanium-oxygen solid solution regions were detected around all the copper particles and this phases probably inhibit the oxidation of copper which is favorable result for aim of study. For the Al containing coatings, possible titanium aluminum intermetallic compounds were detected around aluminum particles. Moreover, titanium-zinc intermetallic compound and preservation of metallic zinc were observed. Lastly, particle boundaries were established as settlement places for iron oxide particles. It is understood from the result of X-ray diffraction analyses; before thermal oxidation only peaks of feedstock elements were determined which proves no chemical reaction during deposition (except iron oxide it may be because of presence less than detachable amount 3 wt. %.) took place. On the other hand, after thermal oxidation, all of the coatings commonly have titanium dioxide (TiO_2) in rutile form and alfa titanium, which detected probably under oxide layer by the penetration of x-rays during test. Furthermore, roughness measurements are done before and after thermal oxidation and 5-6 times increment were observed. This increment in roughness provide the bio-activity of the coating via increasing the interaction of the surface and the surrounding tissues.

Cross sectional and surface hardness, measurements were executed with Vickers hardness and depth sensing micro-nano hardness tester with the Vickers indenter under the load of 25 g and 100 mN respectively. All the coatings showed similar hardness values; before thermal oxidation around 80 $HV_{0.025}$, after thermal oxidation from the crossection around 450 $HV_{0.025}$ from the surface around 900 HV. This results showed that, different kind of additives did not directly affect the hardness of coatings and/or oxide layer. Tribological performance of coatings and substrate were performed under 1N load for 25m sliding distance in dry, serum and simulated body fluid (SBF) sliding conditions. While for the substrate, significant wear track was obtained, for the coatings wear tracks could not be detected by profilometer. Only trimming of rough surface was observed and depth of tracks were not possible to measure on profilometer. These results also were supported by optical micrograpghs of worn surfaces of coatings and alumina balls. Surface of counter bodies are generally clean with the existance of some wear scratches and these observations may thought just simple sliding were occur between the coating and alumina balls for all the cases. Comparative steady state friction coefficients for coatings and substrate were obtained after wear test and results are showing in dry sliding conditions coatings present lower value than substrate in contrary to serum and SBF environment. This behavior may be explain with chemical reaction on the surface of coating in liquid media and extreme contact pressures (around 840 MPa). Lastly, when the coatings individually compared with each other's, Zn containing coatings exhibit the lowest steady state friction coefficient due to possible lubricant effect of metallic zinc or/and zinc-titanium intermetallic compound.

When the in vitro bioactivity tests were on concern, all the coatings showed high bio activity after 4 weeks of immersion in SBF. SEM micrographes of the surfaces demonstrate the formation of structures in the same morphology as hydroxyapatite. Among all four different composition, copper containing coating showed earlier interaction with SBF, as a result hydroxyapatite like structures formed even after 1 week of immersion.

In general, mechanical properties and bioactivity of ASTM F 75 grade cobalt-chromium alloys were improved by the formation of titanium based multilayered coating via sequential application of cold gas dynamic spray and thermal oxidation. These observations show promising future for possible biomedical application of cobalt chromium alloys without sacrificing superior properties.

SOĞUK GAZ DİNAMİK PÜSKÜRTME YÖNTEMİYLE ÜRETİLMİŞ TİTANYUM ESASLI KAPLAMALARIN KARAKTERİSTİĞİ

ÖZET

Sentetik malzemeler arasında metalik biyomalzemeler en yaygın kullanılan mühendislik malzemeleridir. Metalik biyomalzemeleri diğer malzemelerden ayıran en önemli özellikleri; statik ve dinamik yükler altında yüksek mukavemetli olmaları ve yeterli miktarda gösterdikleri korozyon ve aşınma dirençleridir. Kobalt-krom esaslı metalik biyomalzemeler ise, yüksek mukavemet ve korozyon dirençlerinden dolayı, titanyum alaşımları ve paslanmaz çelik malzeme gruplarıyla beraber biyomedikal alanında en çok tercih edilen metalik biyomalzemelerdendir. Bu alaşım grubunun korozyona karşı dirençli olması içerdiği krom sayesinde yüzeyinde doğal olarak oluşan oksit tabakasından kaynaklanmaktadır. Belirtilen üstün özelliklere sahip olmasına rağmen, zaman içerisinde gerçekleşen bölgesel korozyonlar ve yüksek yük altında çalışan implant uygulamalarında görülen aşınma sonucu, bu koruyucu oksit tabaka zarar görmekte, istenmeyen metalik iyon salınımları, insan vücudu için zararlı olmakta ve implantın ömrünü 10-12 yıl seviyelerine düşürmektedir. Bunun sonucu olarak, yüksek maliyetli ve acı eşiği yüksek olan implantasyon operasyonlarının tekrarlanması kaçınılmaz bir hal almaktadır. Ayrıca kobalt krom esaslı malzemelerin bir başka dezavantajı ise, bütün biyolojik özelliklerin bir tanımlaması olan biyouyumluluk açısından zayıf olmalarıdır. Kobalt krom alaşımlarının sahip oldukları üstün özelliklerden ödün vermeden, yüzey özelliklerinin geliştirilmesi için yapılan çalışmalar son yıllarda önemini giderek arttırmaktadır. Bu yüksek lisans tez çalışmasında, kobalt krom esaslı metalik biyomalzemenin yüzeyi, soğuk gaz dinamik püskürtme yöntemi ile titanyum esaslı toz karışımları kullanılarak kaplanmış, ardından biyoaktivitesinin yüksek olduğu bilinen titanyum oksit fazının en dış yüzeyde termal oksidasyon işlemi ile oluşturulması amaçlanmıştır.

Titanyum, yüksek biyouyumluluğu gerekçesiyle püskürtülen toz karışımı içerisinde ana malzeme olarak seçilmiştir. Titanyum yüzeyinde oluşan doğal oksit tabakası biyoaktivite yönünden verimli olsa da, düşük mekanik özelliklerinden dolayı biyomedikal uygulamalarda direk kullanılması mümkün değildir. Literatürde, bu zamana kadar konu üzerinde çalışma yapan araştırma grupları, mikro ark oksidasyon gibi biriktirme ve termal oksidasyon gibi difüzyon esaslı yüzey modifikasyon yöntemleri ile daha stabil ve dayanıklı bir oksit tabakası elde etmek için çaba sarf etmişlerdir. Titanyum-oksijen ikili denge diyagramına göre, oksidasyon reaksiyonu 300 ^{o}C sıcaklığın üzerine çıkıldığı takdirde başlamaktadır. Termal oksidasyon işlemi özelinde, yüksek proses sıcaklıkları daha kalın bir oksit tabakasının oluşmasını sağlamakla beraber bu oksit tabakası altında bir oksijen difüzyon tabakasının oluşmasına da sebep olur. Ayrıca bu oksijen difüzyon tabakası sayesinde, sert- kırılgan oksit yüzey ile ana malzeme arasında daha yumuşak bir sertlik geçişi sağlanırken bu durumun aşınma direncinin de artmasına yardımcı olduğu bilinmektedir.

Yüzey modifikasyon işleminin ilk aşamasında, soğuk gaz dinamik püskürtme yöntemi tercih edilmesinin ana nedeni, kaplama işleminin kolay ve yüksek verimlilikte

olmasıdır. Ayrıca, kaplama sırasında ulaşılan proses sıcaklıkların diğer termal sprey yöntemlerine göre çok daha düşük seviyelerde olması püskürtülen tozlar ile altlık malzemesi arasında herhangi bir kimyasal reaksiyonun gerçeklemesini olanaksız hale getirmektedir. Buna ek olarak, kaplama işlemi sırasında çok yüksek kinetik enerjiye sahip olan partiküllerin altlık malzemesi yüzeyine çarpması sonucu biriktirilen kaplama plastik deformasyondan dolayı altlık malzemesine göre daha yüksek sertlik değerleri elde edilmesine imkân sağlar.

TÜBİTAK tarafından 214M246 proje numarası ile desteklenen proje kapsamında gerçekleştirilen yüksek lisans tez çalışması, titanyum esaslı kaplamalar içerisine yapılan eklentilerin kobalt krom malzeme yüzeyine olan etkilerini incelenmektedir. Bu bağlamda, farklı oranlarda titanyum, alüminyum, çinko, bakır ve demir oksit (manyetit formunda) içeren toz karışımları ASTM F75 kalite kobalt krom alaşımı üzerine püskürtülmüş, elde edilen kaplamalar yüzeyde biyoaktivitesi yüksek olduğu bilinen titanyum oksit tabakası oluşturulması için 600 ^{o}C de 60 saat süreyle termal oksidasyon işlemine tabi tutulmuştur.

Üretilen kaplamaların karakterizasyonu, yapısal karakterizasyon, mekanik özelliklerin belirlenmesi ve biyolojik testler olmak üzere üç ana başlık altında incelenmiştir. Yapısal karakterizasyon kapsamında, X ışınları difraksiyonu, optik mikroskop, çizgi ve alan enerji dağılım analizlerini kapsayan taramalı elektron mikroskobu incelemeleri, termal oksidasyon öncesinde ve sonrasında yüzey pürüzlülüğü ölçümleri gerçekleştirilmiştir. Öte yandan, mekanik özelliklerin tayini için kaplama kesitinden ve oksit tabakasının yüzeyinden sertlik ölçümleri, kuru serum ve yapay vücut sıvısı içerisinde aşınma testleri gerçekleştirilmiştir. Deneysel çalışmaların son bölümünde ise, elde edilen yüzeyin biyolojik özelliklerinin belirlenmesi için biyoaktivite testleri yapılmıştır.

Yüksek lisans tez çalışmasının başlangıcında, ASTM F75 kalite kobalt krom alaşım malzemesi altı ayrı kompozisyonda hazırlanan toz karışımlarının yüzeye püskürtülmesiyle kaplanmıştır. Bu toz karışımları sırasıyla, ağırlıkça % 92 Ti - % 5 Cu- % 3 Fe_3O_4, % 94 Ti - % 3 Cu- % 3 Fe_3O_4, % 95,5 Ti - % 1,5 Cu- % 3 Fe_3O_4, % 87 Ti - % 8 Al- % 5 Zn, % 89 Ti - % 8 Al- % 3 Fe_3O_4, % 84 Ti - % 8 Al- % 5 Zn -% 3 Fe_3O_4 içermektedir. Karışımlar içerisine konulan alüminyum, düşük plastik deformasyon kabiliyetini sahip titanyumun yüzeye tutunmasını sağlamak için kullanılmıştır. Çinko ve bakırın antibakteriyel ajan olarak yapı içerisinde yer alması planlanırken, manyetit formundaki demir oksit partikülleri hem biyoaktiviteyi arttırmak hem de üretilen kaplamaya farklı kullanım alanları kazandırması için tercih edilmiştir. Daha önce de belirtildiği gibi soğuk gaz dinamik püskürtme yöntemi ile kaplanmış olan altlık malzemeler 600 ^{o}C de 60 saat süreyle termal oksidasyon işlemine tabi tutulmuştur.

Karakterizasyon çalışmaları, bakır içeren kaplamalar için kesit optik mikroskop incelemeleri ile başlamıştır ve elde edilen sonuçlar ışığında, yapı içerisinde azalan bakır oranına bağlı olarak, yüksek oranda poroziteler ve düzensizlikler meydana geldiği belirlenmiş ve kompozisyonlar arasında ağırlıkça % 5 bakır içeren ve % 92 Ti - % 5 Cu- % 3 Fe_3O_4, kompozisyonundaki toz karışımı kaplama için en uygun kompozisyon olarak tespit edilmiştir. Bakır içeren kaplamalar için yapısal karakterizasyon çalışmaları, mekanik ve biyolojik testler bu kompozisyondaki toz karışımı ile üretilen kaplamalar üzerinde gerçekleştirilecektir.

Taramalı elektron mikroskop çalışmalarında bütün kompozisyonlar için termal oksidasyon öncesinde yapı içerisinde yok denebilecek kadar az miktarda porozite tespit edilmiştir. Öte yandan, bu oran termal oksidasyon işlemi sonrasında bir miktar artarken, işlem sonrasında yaklaşık 2 µm kalınlığında stabil bir oksit tabakası oluştuğu görülmüştür. Çizgi ve alan enerji dağılım analizleri toz karışımı içerisine eklenen ikincil ve üçüncül eklentilerin tüm yapı ve oksit tabakasına homojen bir şekilde dağıtıldığı gözlemlenmiştir. Yine bütün kaplama kompozisyonları için, oksijenin kaplamaların içlerine kadar difüze olduğu ve özellikle titanyum ile katı çözelti bölgeleri oluşturduğu görülmüştür. Bakır içeren kaplamalar özelinde, titanyumun oksijene olan afinitesinin bakıra göre daha yüksek olmasından dolayı bakır partikülleri etrafında titanyum-oksijen katı eriyik bölgelerinin oluşması termal oksidasyon işlemi sonrasında bakır partiküllerinin metalik özelliğini korumasına sebep olmuştur. Bakır partiküllerinin oksitlenerek vücut için toksik olan bakır oksit halini almaması çalışmanın hedeflerini desteklemektedir. Alüminyum içeren tüm kaplamalarda ise, titanyum ve alüminyum arasında gerçekleşen kimyasal reaksiyonlar sonucu titanyum alüminyum intermetalik bileşikleri oluştuğu düşünülmektedir. Çinko içeren kaplamalarda çinko-titanyum arasında gerçekleşen kimyasal reaksiyon sonucunda ise muhtemel bir intermetalik bileşiğinin oluşumundan söz edilebilirken, metalik çinkonun da yapı içerisinde varlığını devam ettirdiği gözlemlenmiştir. Demir oksit eklentisinin yapı içerisindeki yerleşme bölgeleri olarak, partikül sınırları belirlenmiştir. Buna neden olarak, püskürtme sırasında kırılgan demir oksit partiküllerinin ufalanması gösterilebilir. X ışınları difraksiyonu sonuçlarına bakılacak olursa, termal oksidasyondan önce tüm kaplamalar için yüzeye püskürtülen toz karışımları içerisindeki demir oksit eklentisi dışında tüm malzemelere ait pikler tespit edilmiştir. Bu sonuç kaplama işlemi sırasında püskürtülen tozlar arasında herhangi bir kimyasal reaksiyon gerçekleşmediğini göstermektedir. Demir oksit eklentisinin tespit edilememesi, yapı içerisindeki miktarın tespit edilebilir minimum limit olan %3 oranından daha az olması ile açıklanmaktadır. Termal oksidasyon işleminden sonra ise tüm kaplama kompozisyonlarında, ortak olarak titanyum oksitin rutil fazına, x ışınlarının oksit tabakası altına nüfuz etmesi sonucu titanyumun alfa çözeltisine ait piklere rastlanmıştır. Termal oksidasyon öncesinde ve sonrasında yapılan yüzey pürüzlülüğü ölçümleri, titanyumun oksidasyonun doğal bir sonucu olarak bu işlemin pürüzlülüğü 5-6 kat oranında arttırdığını göstermektedir. Yüzey pürüzlülüğü yüksekliğinin biyoaktiviteye yaptığı olumlu etkiden dolayı bu sonuç çalışmanın hedefleri doğrultusunda tatmin edici bir sonuç olarak algılanabilir.

Zımparalanmış ve parlatılmış kesitten 25g yük kullanılarak micro Vickers sertlik cihazıyla ve termal oksidasyon sonrası yüzeyden 100 mN yük kullanılarak derinlik hassasiyetli nano-mikro sertlik cihazı ile yapılan sertlik ölçümleri, termal oksidasyon işlemi öncesinde 80 $HV_{0.025}$ olan kesit sertliğin termal oksidasyon sonrasında 450 $HV_{0.025}$ değerlerine ulaştığını göstermiştir. Öte yandan tüm kaplamalar için oksit tabakasının sertliğinin 900 HV civarında olduğu görülmüştür. Kaplama kompozisyonuna yapılan eklentilerin bu değerlere direk bir etkisi tespit edilememiştir. 1 N yük altında 25 m kayma mesafesinde, kuru, serum ve yapay vücut sıvısı içerisinde gerçekleştirilen aşınma test sonuçları, üretilen bütün kaplamaların her koşulda altlık malzemesine göre aşınmaya daha dirençli olduğunu göstermiştir. Serum ve yapay vücut sıvısı içerisinde yapılan testlerde kaplamalar için ortalama sürtünme katsayıları yüksek değerlerde de olsa, test sonrasında iki boyutlu tarama çalışmalarında herhangi bir rasyonel değere ulaşılamaması, aşınma testi sırasında karşı yüzey olarak kullanılan alümina topun kaplamaların sadece yüzey pürüzlülüğünü azalttığı sonucunu doğurmaktadır. Sıvı ortamlarda sürtünme katsayılarının yüksek olmasına sebep olarak, titanyum oksit ile tuzlu çözeltiler arasında gerçekleşen kimyasal reaksiyonlar gösterilebilir. Öte yandan, çinko içeren kaplamalar özelinde, yapı içerisinde bulunan metalik çinko ve/veya titanyum-çinko intermetalik bileşiklerinin muhtemel yağlayıcı etkisinden dolayı kuru ortamda elde edilen çok düşük sürtünme katsayısı değerleri bu kaplamaların düşük sürtünme katsayılı mühendislik uygulamalarında kullanılabileceğini düşündürmektedir.

1 ve 4 hafta yapay vücut sıvısı içerisinde biyo aktiviteyi belirlemek amacıyla bekletilen kaplamalardan alüminyum içerenlerin yüzeylerinde 4 hafta sonrasında, hidroksiapatit

Morfolojisine sahip yapılar elekton mikroskobu vasıtasıyla belirlenmiştir. Öte yandan, bakır içeren kaplamalar yapay vücut sıvısı ile daha önce etkileşime girip, 1 hafta sonrasında bile bu yapıların oluşmasına olanak sağlamıştır.

Sonuç olarak, ASTM F75 kalite kobalt krom altlık malzemesi üzerine, titanyum esaslı çok katmanlı kaplamalar soğuk gaz dinamik püskürtme ve termal oksidasyon işlemlerinin ardarda uygulanması sonucu üretilmiş ve bu yöntemlerle altlık malzemesinin mekanik ve biyolojik özelliklerinin geliştirilebileceği tespit edilmiştir.

1. INTRODUCTION

Cobalt-Chromium alloys are one of the most commonly used metallic biomaterials with titanium alloys and stainless steels, owing to high mechanical properties (such as high dynamic and static strength and wear resistance) and high corrosion resistance. Hence, this alloy group have been used for implantation in recent years especially for load bearing implants for instance, on femoral ball on hip joint implants or knee joints [1-4]. Although, having these superior properties, their poor osteointegration properties and low biocompatibilities are the biggest disadvantages for biomedical applications [5]. Beside, for the implants working under high metal-metal contact pressure, ion releasing from the worn surfaces limit the service life of this alloy group up to 10-12 years and necessitate to painful reimplantation surgeries [6]. For that reasons, there are many studies in the literature aimed to improve biological mechanical properties of surfaces.

In the recent master thesis study, as a part of research project supported by TUBITAK (Project No: 214M246), feedstock containing titanium, aluminum, copper, zinc and iron oxide in magnetite form were prepared at different ratios and deposited on to ASTM F75 grade cobalt-chromium alloy by cold gas dynamic spray process. Then, cold sprayed alloys were thermally oxidized at 600 ^{o}C for 60 hour in order to obtain stable bioactive titanium based oxide layer on the outermost surface with different biological behaviors respect to compositions. In brief, general objectives of the study; obtain the better surface behavior by improvement on biological and mechanical performance of ASTM F75 grade cobalt-chromium alloy without sacrificing superior properties. Moreover, different materials were added in to composition of coating in order to determine influences on biological and mechanical behavior of coating. Titanium was preferred as a base material of coating, due to well-known high bioactive oxide film on the surfaces which form naturally. Although, having closest elastic modules to the human bone and high corrosion resistance, this natural oxide layers cannot preserve the stability against to any wear condition. Hence, in the literature lots of study focused on the development of more stable oxide layers on the surface of titanium and titanium alloys by application of diffusional or depositional surface modification technique [7, 8]. Moreover, by the modification of the surfaces ion releasing problems can be suppressed. Additionally, during formation of oxide layers surface roughness are increasing and this natural outcome, provide increment on the bioactivity of the surfaces via increasing the interaction of the surface and the surrounding tissues. Thermal oxidation process, stands out amongst other oxidation techniques, due to simplicity and high efficiency. Moreover, forming oxygen diffusion zone beneath the brittle oxide layer allows smooth transition on hardness and increase the wear resistance of coating [9, 10]. Beside the mechanical properties, bioactivity and antibacterial properties are worth-stressing subject for biomaterials. In that respect, in the present study copper and zinc were added to feedstock compositions as an antibacterial agent and iron oxide particles (in a magnetite form) was enrolled to improve bioactivity and enlarge the application area of coatings such as magnetic resonance imaging contrast agent, targeted drug delivery due to magnetic behavior.

Within the scope of recent master thesis study, titanium based feedstock with different additives are deposited by cold gas dynamic spray process. Subsequently, thick and stable oxide layer is formed by the application of thermal oxidation process. Structural characterization of coatings have been invetigated by optical and scanning electron microscope -including area and line scan energy dispersive X-Ray spectroscopy-, x-ray diffraction analysis and surface roughness measurements. For the mechanical behaviors, hardness measurements, wear tests and pull out tests have been examined. Lastly, in vitro bioactivity test has been performed for the determination of biological properties.

Briefly stated, in this thesis literature review about metallic biomaterials and surface modification of cobalt-chromium alloys are given in the second chapter. Then, experimental methods are presented in third section, followed by results and discussions (forth section). Finally, all the results are concluded in from the master thesis study in fifth section.

2. LITERATURE REVIEW

2.1 Metallic Biomaterials

Biomaterials or in the other word biological materials are used for curing or/and make improvement on functional part of human body. The main purpose of using biomaterials in human body is to change or/and make improvement in any damaged or infected tissue or organ due to any daisies or accident. These material group as can be natural or synthetic [5, 11, 12]. Metallic biomaterials are the most common implant material from syntetic biomaterials. Metallic biomaterials are unrivaled for implant application due to high dynamic and static strength, enough resistance to corrosion, high wear and fatigue resistance. Mechanical properties of metallic materials in biomedical applications are given in Table 2.1 [13]. Also in Figure 2.4, some example of metallic biomaterials are given. The first used metallic material as biomaterials in history is vanadium steel and it was used for fixing broken bones. After development of technology in biomedical industry, iron, chromium, cobalt, titanium, tantalum, niobium, molybdenum and tungsten alloys have started to widely use as an implant materials [14].

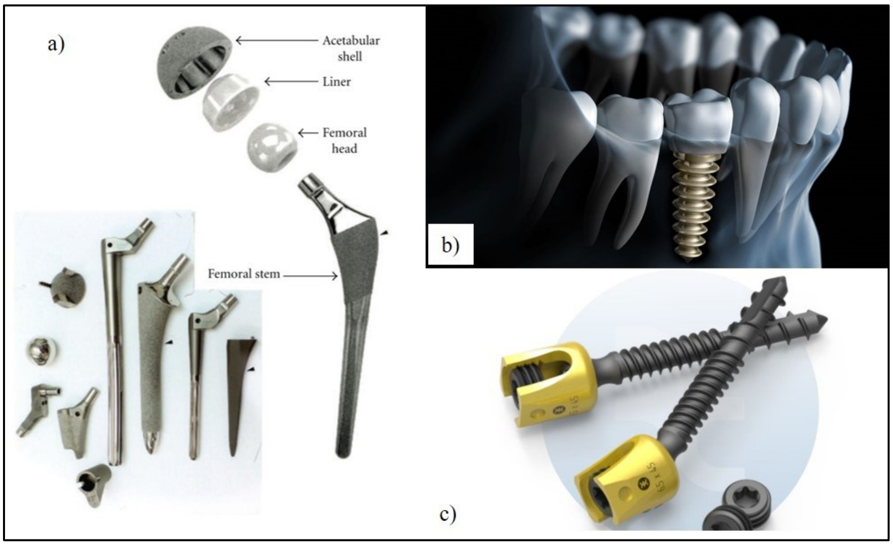

Figure 2.1: Some example of metallic biomaterials a) knee joint implant, b) dental implant, c) bone splinting screws

Average life standard and lifetime of world human population have been increased in last century. In this parallel, hard tissue diseases increase respect to increment in the elder human population as expected. This situation naturally generate the necessity of metallic biomaterials [11, 12]. Beside the mechanical properties, formability is another advantage for metallic biomaterial. It is possible to manufacture basic and complex structures with different kind of manufacturing processes. This advantage enables to implantation process to specific and critical areas of human body such as dental implantations and artificial heart surgeries (mechanically order the rhythm of artificial heart) [15].

Although having these big advantages, in the course of time metallic alloys lose their wear resistance and function because of micro and/or macro motion. After losing this critical resistance, biodegradation of metallic ions as a wear product, causes complications and unfavorable reactions in human body. Tribological interactions in metallic biomaterials also damage the passive and/or active oxide layer on the surface of materials and enable direct contact of metallic surface and tissues or organs. Then this situation decrease the corrosive resistance of metallic biomaterial. Previous studies which focus to biological effect of wear products in human body showed that, during tribological interactions, wear products locate around the implants and inhibit the cell refurbishments and caused the infections. Moreover, in extreme cases, neighbour organs and tissues affect from infections. As mentioned before, in these cases, sole remedy is reiteration of medical attention, which drive patients to unhappiness due to high pain level. In the other respect, when the soluble wear products are concern, high diffusion of metallic ions to the body fluids increase the concentrations and cause different kind of symptoms and/or diseases such as high sensitivity, nervous system disorders, allergic reactions. Again in extreme cases, high concentration of metallic ions in body fluids or/and organs shows toxicity and carcinogenic reactions. Some well-known effect of metallic ions at high concentrations to human body are given in Table 2.2 [16-21].

Cobalt-chromium alloys, stainless steels, titanium based alloys are the most preferred metallic biomaterials. While cobalt-chromium and stainless steels are coming into prominence due to high static and dynamic strength with high corrosion resistance, titanium alloys are favorable due to low elastic modulus and bioactivity.

Table 2.1 : Mechanical properties of most common used metallic biomaterials.

Material	ASTM Standard	Condition	Elastic Modulus (GPa)	Yield Stress (MPa)	Tensile Stress (MPa)	High Cycle Fatigue Stress Limit (MPa)
Stainless Steel	F745	Annealed	190	221	483	221-280
	F55, F56, F138, F139	Annealed	190	331	586	241-276
		Cold Worked 30 %	190	792	930	310-448
		Cold Forged	190	1213	1351	820
Co-Cr Alloys	F75	Cast/Annealed	210	448-517	655-889	207-310
		Hot Isostatic Pressed	253	841	1277	725-950
	F799	Hot Forged	210	890-1200	1399-1586	600-896
	F90	Annealed	210	450-650	951-1220	-
		Cold Worked 44 %	210	1600	1896	586
	F562	Hot Forged	232	969-1000	1206	500
		Cold Worked, Aged	232	1500	1795	596-793
Ti Alloys	F67	Cold Worked 30 %	110	485	760	300
	F136	Forged / Annealed	116	896	965	620
		Forged, Heat Treated	116	1034	1103	620-589

Table 2.2: Biological effects of mettallic ions

Metallic Ion	Known Biological Effects
Nickel	Allergic, high sensitivity and carcinogen
Titanium	Bio inert but in high biodegradable situations it caused to pneumonia
Molybdenum	Low cell activity
Aluminum	Epilepsy effects, anomaly and alzheimer
Chromium	High sensitivity, carcinogen, caused to ulcer
Cobalt	Carcinogen, high productivity of erythrocyte
Vanadium	Depression, hearth and kidney daisies
Iron	Allergic and carcinogen

2.1.1 Titanium and titanium alloys

Titanium and its alloys are commonly used in biomedical applications due to high strength/weight ratio, corrosion resistance and most importantly high biocompatibility. Natural passive oxide layer on the surface of titanium and its alloys increase corrosion resistance as well as bioactivity of surface. Bioactive characteristic of surface enables the implantation process and increase compatibility with surrounding tissue. Beside the surface characteristic, titanium and its alloys have the closest elastic modulus (100-120 GPa) in the other word the closest mechanical property to cortical bone (10-30 GPa).

Biological and mechanical properties of Ti–29Nb–13Ta–4.6Zr (TNTZ) and Ti-12Cr alloys have been investigated by Niinomi et al. [23] to generate alternative to the pure titanium and Ti-6Al-4V, which have relatively high elastic modulus. The results show that, Ti–29Nb–13Ta–4.6Zr (TNTZ) and Ti-12Cr have lower elastic modules and composed of non-toxic and allergy-free elements. In near future it is highly expected that, two titanium alloy going to be used as a metallic biomaterial for implants replacing of failed hard tissue.

Geetha et al. [24] reviewed the properties of titanium based metallic biomaterials and gave suggestions to the development area of titanium and its alloys for orthopedic implants. They summarized that, the main challenging problem of titanium alloys is to develop an appropriate microstructure with optimum mechanical properties especially the wear resistance. Nevertheless, in future, if the superior focus made on the areas of development of grater surface properties with the high hardness, increment on the functional lifetime of biomedical implants will be attained.

The recent studies showed that, although having good biological properties such as high biocompatibility, titanium and its alloys are lack of sufficient mechanical properties especially the wear resistance functional longevity.

2.1.2 Cobalt-chromium alloys

Cobalt chromium alloys are started to be used as a metallic biomaterial in biomedical industry in early 40's. Most commonly used composition is consist of cobalt, chromium and molybdenum [15, 25]. Moreover, due to having high dynamic and static strength, they are favorable for implants under load such as hip and knee joints. According to cobalt and chromium binary phase diagram, cobalt and chromium form solid solution up to 65 atm. % cobalt [26]. In addition, it well know from the literature, strength and corrosion resistance of these alloy group depend on concentration of chromium. Furthermore, external molybdenum addition to the system decrease the grain size and naturally increase the strength of material [27].

Common Co-Cr alloys can be examine under four different group respect to manufacturing method and composition; ASTM F75 Co-28Cr-6Mo (cast alloy) ASTM F1537 Co-28Cr-16Mo (high carbon version of F75 wrought alloy), F799 Co-28Cr-6Mo (low carbon version of F75 wrought alloy), ASTM F562 Co-35Ni-20Cr-10Mo (wrought alloy).

ASTM F75 cast Co-Cr-Mo alloy also known as Vitallium and Haynes 21, is very important material for implantation process. The most characteristic properties of this alloy group is corrosive resistance due to high content of chromium in the elemental distribution. Passive chromium oxide (Cr_2O_3) layer on the surface, protect the material in corrosive media especially in chorine containing environment. Also high content of carbon precipitate on the grain boundaries in the form of M23C6, M7C3 and M6C carbide (where M may represent cobalt, chromium and molybdenum) increase the wear resistance. According to desirable conditions ASTM A799 or ASTM F1537 wrought alloys, which may be the alternative to the ASTM F75 cast Co-Cr-Mo alloy.

Patel et al. [28] studied relationship between forming route, microstructure and tribological performance of Co-Cr-Mo alloys In the study, they have evaluated two conventional alloys (ASTM F75 and ASTM F1537) and a spark plasma sintered (SPS) alloy. The results show that, F75 and F1537 has similar microstructure while F75 has slightly higher hardness and wear resistance compare to the F1537. In the other respect, SPS alloy has the highest hardness and wear resistance with very different microstructure from all. Nevertheless, other mechanical properties such as tensile/compression strength, fatigue performance should be performed for SPS alloy for orthopedic uses.

When the biomedical application of Co-Cr based alloys are concern, they are commonly preferred for femoral ball on hip joint implants or other surface bearing implants due to resistance to metal-metal contact with high toughness and wear [12]. Then again, for instance F1058 Co-Cr alloys usually used for dental applications such as dental bridged and implants due to elastic recovery potential in the other word spring back property [29, 30].

2.1.3 Stainless steels

Steels which has more than 10.5 wt.% chromium in chemical composition are named as stainless steels. Due to existence of chromium and about two nanometer thick natural chromium oxide layer on the surface, this alloy group is resistant to corrosion. Moreover, it is possible to encourage corrosion resistance and mechanical properties of stainless steels by addition of different metals in to composition such as molybdenum or tungsten [12].

Only 1 % of world stainless production in world market is used for biomedical applications. Beside the implantation processes, stainless steels are attractive material for medical instruments. Nevertheless, when the implantation process is concern, more strength and corrosive resistant grade of stainless steels and special manufacturing methods are preferred.

Stainless steels can be divided to the five different category according to crystal structure and hardening mechanisms; ferritic, martensitic, austenitic, austenitic-ferritic, precipitation hardened. From all, austenitic stainless steels are mostly preferred due to high dynamic and static strength, high corrosion resistance and high formability. Main compounds of austenitic stainless steels are chromium and nickel. While chromium provides corrosion resistant due to chromium oxide formation, nickel provides stability of austenitic structure at room temperature. In recent years, low carbon version of 316 grade austenitic stainless steels (316 L) are the most commonly used material for biomedical applications [31]. Additionally these grades are favorable due to low production cost compare to the titanium or cobalt-chromium alloys. However, the main disadvantage of this material group is low surface strength. Stainless steels can not provide wear resistance in joint implant and after some time, this situation caused ion oscillations. In that respect, there are several studies in literature focused on surface modification of stainless steel to improve wear resistance and biological properties.

Gopi et al. [32] coated to surface of pretreated 316L with hydroxyapatite by electro deposition method and blocked the ion oscillations. In addition, successful formation of hydroxyapatite phase improved the bioactivity of surface.

Pauline et al.[33], modified the surface of 316 L by sol gel coating method. The examinations showed that, strontium added nano porous titanium oxide coatings provides higher bioactivity and corrosion resistance.

Sutha et al. [34], investigated effect of zinc- hydroxyapatite-chitosan composite coating on biological properties and corrosion behavior. In that respect, they have formed coating on 316 L stainless steel alloy by spin coating method and found that composite coating has higher bio activity due to hydroxyapatite and showed antibacterial property due to zinc with high corrosion resistance.

2.2 Surface Modification of Metallic Biomaterials

Surface modification technologies can be divided into two different group, depositional surface modifications which aims to form new layer of material with different microstructure and properties; diffusional surface modification which aims to modify and/or improve the properties of main material on the surface.

2.2.1 Depositional surface modification

Developed technologies on surface depositional surface modification area provide to combine properties of two different material with very different characteristic.

Arslan et al. [35] coated the surface of aluminum with micro arc oxidation process and combine properties of aluminum oxide and aluminum. Result of study showed that, they have achieved to form hard, wear resistant ceramic coating on the surface without sacrificing main properties such as high strength/weight ratio.

Krząkała et al.[36], reviewed the literature concerning the surface modification of implants composed of titanium and titanium alloys by plasma electrochemical oxidation (PEO), also known as micro-arc oxidation (MAO). As a conclusion, they have demonstrated that, in most cases, this coating enhances the bioactivity of surface and enable the usage of these material in biomedical applications for improving bone adhesion.

Nguyen et al. [37], examined the effect on the ingrowth and osteoconductivity properties of sol gel formed calcium phosphate coatings coating on porous surfaced Ti alloy. After in vivo biological tests, they have found that, the implants with sol gel coatings have significantly greater implant-bone contact respect to the uncoated alloy.

However, it should be noted that, the main disadvantage of deposition processes poor bonding between coating and substrate. For instance, Harman et al. [38] examined the TiN coated Ti-6Al-4V hip joints and they showed that delamination of nitride coating cause early failure of implant.

2.2.2 Cold gas dynamic spray technique

Cold gas dynamic spray process (CGDS) was developed by Russian scientist Anatolii Papryin and his colleagues in the middle of 80's. Papryin and his colleagues have been succeed to deposit several number of pure metals, alloys, polymers and composites on different kind of substrate [39-41]. Schematic illustration of CGDS seen in Figure 2.3.

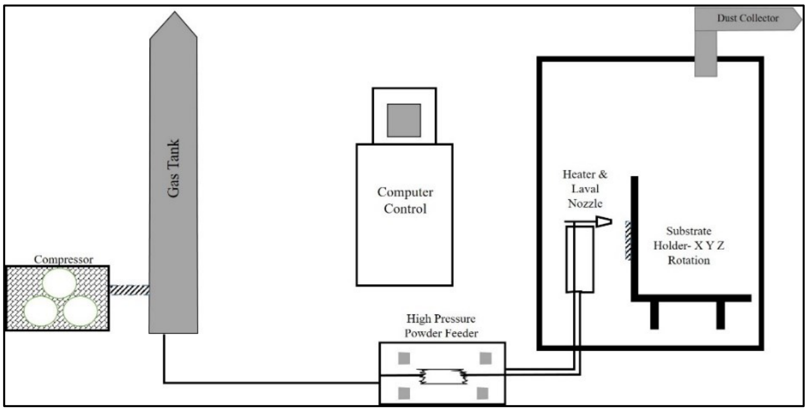

Figure 2.2 : Schematic illustration of CGDS

In CGDS, particles (generally under fifty microns) reach to supersonic velocity by the effect of compressed gas- which are fed to the system- and the design of Laval nozzle (Figure 2.4) [42].

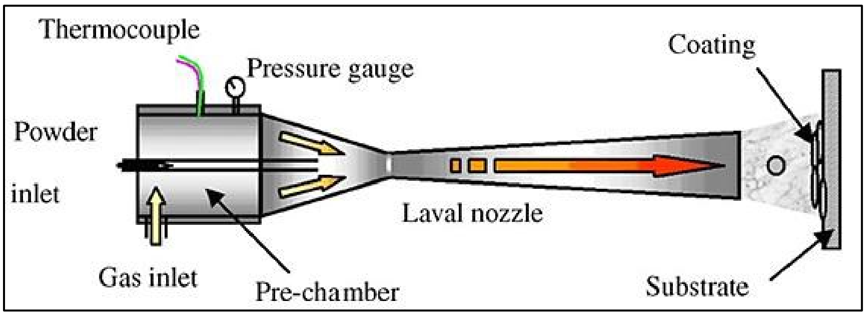

Figure 2.3 : Schematic illustration of Laval Nozzle

Accelerated particles (300-1200 m/s) exit from the Laval nozzle and impact to the surface of substrate with high momentum and form the first layer in stage 1 in Figure 2.4. During the process, powders continue to attach to the material which adherent to the surface of substrate later in Stage 2. Because of this mechanism, relatively thick homogenous coating with small amount of porosity and distribution of grain size are provided (Stage3-4) [39, 43, 44].

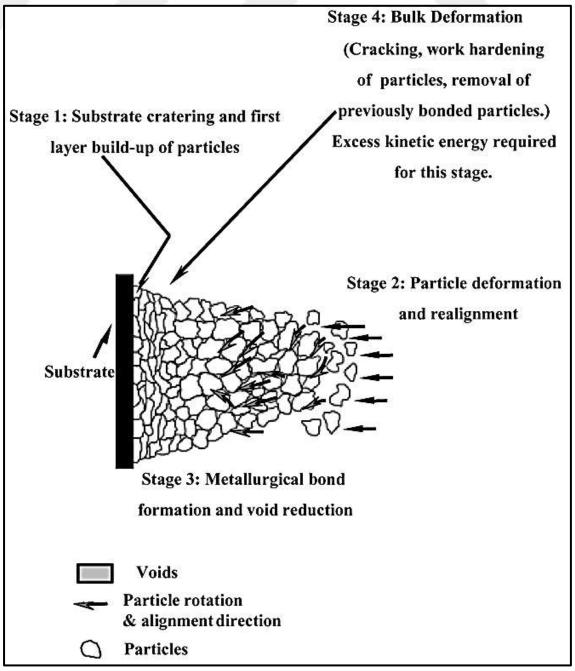

Figure 2.4 : Deposition mechanism of titaniums in CGDS

Plastic deformation is not the only mechanism for formation of coating on substrate. Other mechanism can be align as adhesion, erosion, ballistic at high velocity and cold spraying at mid velocity. Mechanism change according to the particle size is given in

Figure 2.5. It is clear that, when the particle size change between 10-100 μm, most efficient mechanism, which is high velocity impact (300-1200 m /s), takes place.

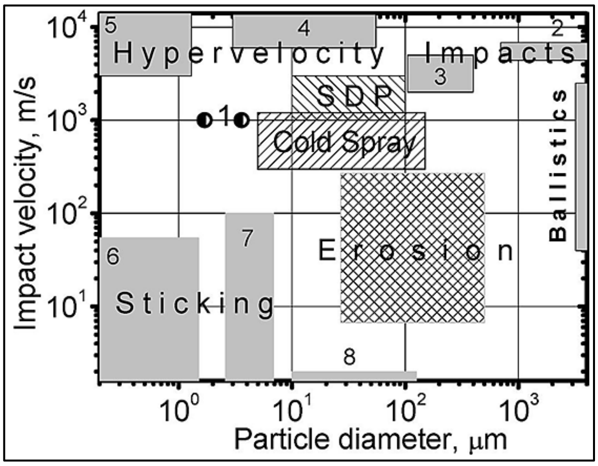

Figure 2.5 : Influence of particle size to the impact velocity change[45]

In CGDS, the most important parameter is the velocity of the particles. This parameter, in other word deposition efficiency is directly related with some parameters like, type of gas, temperature, pressure, density, particle size and morphology of powder. Moreover, Laval nozzle design is another parameter, which change the acceleration of particles according to the given equation below. In equation 2.1, M is the Mach number which described as ratio of nozzle exit area (A) to the minimum cross sectional area (A^*). Also, Mach this Mach number equal to the ratio of gas velocity (V) and sound velocity (c).

$$\frac{A}{A*} = M = \frac{V}{c} = \frac{V}{\sqrt{\gamma RT}} \quad (2.1)$$

R: Gas constant (universal gas constant / molecular weight of process gas)

T: Gas temperature

γ: Ratio of specific heats of gases (C_p / C_v)

In general theory, other parameters (temperature of process gas, pressure, particle size etc.) are set constant, the powder velocity increase when Mach number increase. Nevertheless previous studies showed that, after some specific level velocity of particles reach the maximum [42]. Process gases in CGDS technique provide to reach to the hypersonic sound velocity. It is possible to reach higher velocities, when the molecule weight decrease and/or specific heat ratio increase pursuant to the gas dynamic law (Equation 2.1). Common used gases in CGDS of titanium is given in Table 2.3 regards to maximum velocity, density, reactivity and price [46].

Table 2.3: Commen used gases in CGDS of titanium

Process Gas Type	Speed (m/s)	Noble or Reactive	Density (Kg/m_3)	Price
Air (80 % N_2+ 20 % O_2)	343	Reactive	1.225	Cheap
N_2	349	Non-Reactive	1.185	Cheap
H_2	1303	Reactive	0.085	Expensive
Ar	319	Noble	1.69	Expensive
He	989	Noble	0.168	Very-Expensive

Stenkiste et al. [47] investigated the effect of inlet temperature to the particle velocity with different size of particles and revealed that, at high inlet temperatures it is possible to reach higher velocities. Furthermore, pressure change in laval type nozzle directly affect the type of flow (laminar or turbulent) and velocity. In that respect, particles reach higher velocities at higher pressure differences. Other parameter, which affect the output velocity of particles, is morphology of powder. Fukumoto et al. [48] were showed in their studies yhat, the powders with higher density and higher particle size cannot reach the sufficient velocity level in other word sufficient kinetic energy and escape from system without deposition. On the other hand, powders with lower particle size and density reach hypersonic velocity level and high kinetic energy and deposit to the surface of substrate [45, 49, 50].

CGDS technique is relatively new technology compare to the other surface modification techniques. Nevertheless, most of metals, alloys and composite materials can easily coat with CGDS technique with high efficiency. Recent studies showed that, it is possible to reach really high deposition efficiency if;

- Oxygen amount in process atmosphere is reduced to the minimum,
- Residual stress is reduced in powder mixture,
- Optimum spraying parameters is provided [40].

Biggest advantage of CGDS technique is formation of coating without any chemical reaction and/or melting. For that reason, CGDS is the one of most sufficient technique for surface modification of heat sensitive metals because of high affinity to oxygen such as titanium. Moreover, due to plastic deformation during process, it is possible to have coating harder that substrate material.

On the other hand, as mentioned before main deposition mechanism of CGDS technique is plastic deformation of particles. In that respect, it is not possible to use pure ceramic powders or the metals, which has lower plastic deformation ability such as titanium and zinc [40]. Only way to use these materials is mixing with softer metals like aluminum or copper. Therefore, in this study titanium powder is mixed with copper and aluminum.

2.2.3 Cold gas dynamic spray of titanium

Coating of metallic biomaterials such as Co-Cr or Ti alloys is very attractive topic of research in recent year studies due to less biocompatibilities. Moreover, cold gas dynamic spray is one of the most preferred technique coating of these alloys because of simplicity and effectiveness.

Zhou et al. [51], investigated electro chemical behavior of cold sprayed pure Ti and hydroxyapatite/titanium (HAP-Ti) composite in Hanks' solution. As a result, porous structured (which can be considered as an advantage for promoting bone growth onto the implants) and rough Ti based coating manufactured on Cp titanium substrate with good bonding on interface. Additionally, improved mechanical and biological properties are promising for future biomedical applications.

Sun et al. [52], fabricated porous titanium coating on titanium by cold gas dynamic spray and vacuum sintering. By the formation porous structure, elastic module of titanium has been decreased and matched with the cortical bone, which enables to use this material under load bearing applications su ch as hip or knee joints.

2.2.4 Diffusional surface modifications

In the other respect, with the diffusional surface modification techniques it is possible to change microstructure and surface properties of main material. Localized hardening techniques (carburizing or nitriding) and thermal oxidation are the most commonly used technologies.

Guleryuz et al. [7] studied the effect of thermal oxidation on the corrosion and corrosion-wear behavior of Ti-6Al-4V. They have concluded that, thermally oxidized Ti–6Al–4V alloy exhibited excellent resistance to corrosion. Additionally, because of thermal oxidation the material achieved 25 times higher wear resistance than the untreated alloy.

Bou-Saleh et al. [53], applied cyclic linear potentiodynamic polarization technique to the 316 LVM quality stainless steel for biomedical application. Because of potential between hydrogen and oxygen, they have formed passive surface film, which protect the material against to the pitting corrosion.

The main disadvantage of diffusional surface modification techniques is limitation on improving surface properties, especially for biomedical application, if the main material is not favorable for human body it is not possible to use as biomaterial even after surface modification.

In that respect, in the recent master thesis study, depositinal and diffusional surface modification techniques (cold gas dynamic spray and thermal oxidation) sequentially applied to combine advantage of both process and achieve multilayer coating on the surface of ASTM F75 grade Co-Cr-Mo alloy.

2.2.5 Thermal oxidation process

Metal oxides form in oxidation of metals because of chemical reaction between metal and oxygen. Even, oxidation in metals starts without any extra effort, in some cases it can be started with thermal energy or electrical current. In the case of thermal oxidation, heat input to the system, accelerate the diffusion rate and cause the formation of oxide layer on the surface. In electrolytic oxidation processes under stable potential condition, reduction in anode and oxidation in cathode form the oxide layer. Moreover, it is known from the open literature that, the oxides that formed with these two different techniques show different characteristic [7].

2.2.6 Thermal oxidation of titanium

Titanium as a metallic material is well known with high affinity to the oxygen. Even at room temperature, 10 nm thick passive oxide layer easily form on the surface of this material. Nevertheless, this protective oxide layer is not resistant against to the any mechanical effect and easily pull out from the surface then caused the direct contact of metallic surface with open environment. Due to this direct interaction between metallic surface and environment, titanium and its alloys loses their corrosion resistance, bioactivity and become ordinary material. Under the light of this knowledge, sustainable oxide formation on the surface of titanium is one of the attractive research interest in recent years. In that respect coating processes like thermal oxidation, anodic oxidation, micro-arc oxidation etc. are mostly used to answer this purpose [54-56].

Thermal oxidation is the most popular thermochemical coating technique for the oxidation of titanium and its alloys. When the oxidation process applied over 200 °C, thickness of the oxide layer on the surface increase with respect to temperature and process time period. It is known that, titanium has seven stoichiometric oxide compound (TiO, Ti_3O, Ti_2O_3, Ti_2O, Ti_3O_2,Ti_3O_5 and TiO_2) and TiO_2 is the most stable from all. Moreover, TiO_2 has three different crystallographic structure such as, rutile, anatase in tetragonal structure and brookite in orthorhombic structure [57]. At higher thermal oxidation temperatures, oxygen atoms diffuse in to the titanium and solid solution region form beneath the oxide layer on the outermost surface. This region known as oxygen diffusion zone and titanium can solve oxygen up to 30 atomic % according to binary phase diagram in Figure 2.6 [58].

Also previous studies showed that, diffusion mechanism increase the hardness of titanium [59]. Diffusion rate of oxygen, consequently hardness gradually decrease respect to the depth and schematic view of this phenomena could be seen in Figure 2.7. Oxygen diffusion zone under the brittle oxide layer increase the wear resistance and highlight the thermal oxidation compare to the other oxidation techniques [60-63].

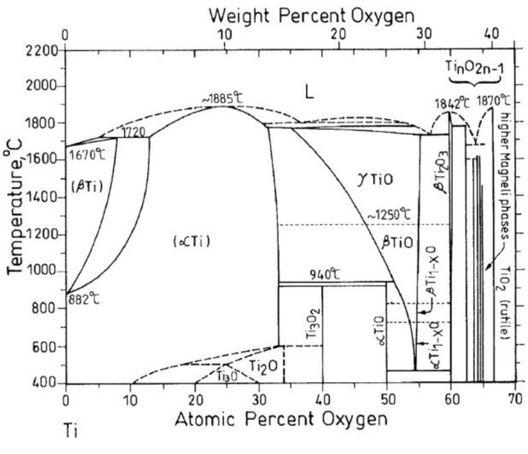

Figure 2.6 : Titanium-Oxygen binary phase diagram

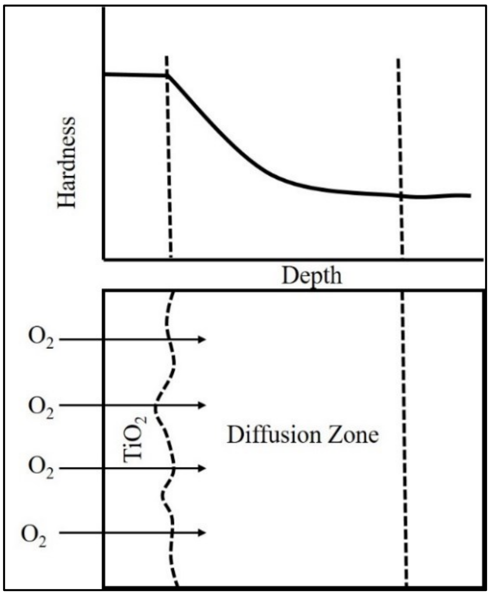

Figure 2.7 : Hardness change of diffusion zone respect to the depth

Furthermore thermal oxidation process is one of the most preferred technique for bioactive oxide layer formation on surface of titanium and its alloys for biological applications [64-66]. Çimenoğlu and his friends have examined the bioactivity of Ti6Al7Nb alloy after thermal oxidation in simulated body fluid and concluded thermal oxidation increase the bioactivity of this alloy [66].

According to this theoretical and practical knowledge, objectives of thermal oxidation of titanium can be listed as;

- Increase the bioactivity of titanium with the formation of oxide layer on the surface,
- Increase the wear and corrosive resistance due to dual effect of oxygen diffusion zone and oxide layer on the outermost surface.

2.3 Surface modification of cobalt chromium alloys

As briefly discussed above, Co-Cr alloys especially F75 grade alloys, have been extremely used in biomedical applications due to well-known favorable properties such as, high wear and corrosion resistance and fatigue strength. Nevertheless, bio inert behavior is the deficiency of these alloy groups. In order to improve biological properties, there are several studies in literature which focused to surface modification of Co-Cr based alloys.

Mani et al. [67] formed self-assembled monolayer on Co-Cr-W-Ni alloy to improve biological properties of surface. After examinations on stability of coating in physiological conditions for seven days, results showed that, Co-Cr alloys could be surface modified by using self-assembled monolayer coating and improved the biological properties for future promising biomedical applications.

Onate et al. [68] have been investigated effect of nitrogen ion implantations and hard coatings (TiN and DLC) on Co-Cr alloy for potential wear reduction applications in human body. On the contrary to other studies, they have executed the wear tests in knee wear simulator and reach the closest conditions to human body. The results demonstrated that, all the surface treatments improve the wear resistance while the most favorable coating from all is diamond like carbon (DLC) coating that reduce to wear about five times and has passed biocompatible tests.

Wei et al. [69] were nitrided the orthopedic materials (Co-Cr alloys and Ti-6Al-4V) in order to enhance lifetime of tribological performance. In the first part of the study, effect of process temperature and manufacturing method on wear resistance of both alloy were observed. In that respect, while forged Co-Cr alloys show much more better performance when nitrided at low and high temperatures and there is no improvement can be observed on cast Co-Cr alloy due to possible microstructural effects.

3. EXPERIMENTS

3.1 Coating Processes

F 75 grade Cobalt-Chromium-Molybdenum alloy with 8 mm in diameter was used as a substrate and composition of the feedstock can be seen in Table 3.1. Samples were grinded with silicon carbide abrasives up to 320 grit, and cleaned with 100% ethanol to provide clean and rough surface for CS process.

Table 3.1: Content of powders mixtures**.**

Number of Feedstock	Compositon of Feedstock (Wt. %)
1	92 wt.% Ti – 5 wt.% Cu – 3wt.% Fe_3O_4
2	94 wt.% Ti – 3 wt.% Cu – 3wt.% Fe_3O_4
3	95.5 wt.% Ti – 1.5 wt.% Cu – 3wt.% Fe_3O_4
4	87 wt.% Ti- 8 wt.% Al – 5 wt. % Zn
5	89 wt. %Ti – 8 wt.%Al – 3 wt.% Fe_3O_4
6	84 wt. %Ti – 8 wt.%Al – 3 wt.% Fe_3O_4 - 5 wt.% Zn

Prepared feedstock were deposited on Co-Cr substrate by using RUSONIC Model K-201 CS equipment (Figure 3.1). 6 bar (600 kPa) inlet pressure of air was used as a process gas and traverse speed were fixed at 5 mm/s for all the cases. Stand–off distance, beam distance and powder feeding rate were set as 10 mm, 2mm and 2 (equipment setting scale of 8), respectively.

Figure 3.1 : RUSONIC Model K-201 CS equipment

In theory of cold gas dynamic spray coating technique, highly accelerated particles are deposited to the substrate as a result of plastic deformation. In this study, pure titanium and iron oxide powder mixture cannot be deposited on ASTM F-75 grade Co-Cr alloy due to low plastic deformability of these materials and limitations of coating equipment. In order to overcome this problem, aluminum or copper (also added for antibicrobial property) having high plastic deformability materials were added to the all powder mixtures with the diferent ratios.

Standard metallographic preparation procedure includes grinding with silicon carbide abrasives up to 2500 grid and mirror polishing with 1-micron silica suspension on Chem. Cloth applied in order to reduce thinkness (to avoid possible pull out during thermal oxidation due to thermal expension differences between coating and susbtrate) and obtain smooth surface before thermal oxidation. After metallographic preparations, all the samples were cleaned with 100% ethanol and place in to NABERTHERM electrically resistant furnace. 600 ^{o}C and 60 hour were chosen as an optimum parameter for the thermal oxidation under the light of previous studies, which has done by Cimenoglu et.al. [66]. CS Coated samples were heated up to 600 ^{o}C with the 5 ^{o}C/min heating rate and cooled down to the room temperature after 60 hour with 1 ^{o}C/min cooling rate due to annihilate the thermal stress failure risk which occur as a result of differences on thermal diffusivity of coating and substrate. Then the oxidized samples were cleaned with 100% ethanol for characterizations.

3.2 Structural characterization

In this section, experimental method for structural survey including microstructural characterization, x-ray diffaraction analysis and roughness measurements will be explained.

3.2.1 Microstructural characterization of coatings

Firstly, microstructural characterization of coated samples with seven different feedstock have performed from the cross-sections before and after thermal oxidation. In that respect, samples were vertically molted, ground (from 320 to 2500 grid abrasive) and polished (with colloidal silica). Samples, which are prepared with standart metallographic procedures, were examined via Leica optical microscope and Philips XL 30 SFEG scanning electron microscope (SEM). During microscopic examinations, interface between substrate and coating, morphological structure of coating and oxide layer on the outermost surface were considered. Additionally, EDX attachment was charged for line and spot-area x-ray surveys. Due to determination of high discontinuity and porosities for the samples that coated less then 5 wt. % copper containing feedstock, advance chracterizations and biological test were perfomed only for selected feedstock compostions (Table 3.2).

Table 3.2: Selected feedstock compositions for advance characterization and biological test

1	92 wt. %Ti – 5 wt.%Cu – 3 wt.% Fe_3O_4
2	87 wt.% Ti- 8 wt.% Al – 5 wt. % Zn
3	89 wt. %Ti – 8 wt.%Al – 3 wt.% Fe_3O_4
4	84 wt. %Ti – 8 wt.%Al – 3 wt.% Fe_3O_4 - 5 wt.% Zn

3.2.2 X-ray diffraction (XRD) analysis

XRD analyses were executed with Cu Kα radiation between the angles of 10◦-90◦ on GBC MMA XRD equipment to identify the different phases in the coatings.

3.2.3 Surface roughness

In order to see effect of thermal oxidation on the surface properties, roughness of coatings before and after thermal oxidation determined by using Veeco Dektak 6M profilometer under 5 mg normal load and for 2000 μm scanning distance.

3.3 Chracterization of mechanical properties

In this section, experimental method for the characterization of mechanical properties will be explained.

3.3.1 Hardness measurement

Overall hardness of the coatings (before and after thermal oxidation), from the polished cross-sections, were determined by Wilson microhardness tester with a Vickers indenter under a load of 25 g. Moreover, after thermal oxidation CSM depth sensing micro-nano hardness tester enrolled with the Vickers indenter and 100 mN testing load for hardness measurements of oxide layer the surface from the surface.

3.3.2 Tribological test

Tribological performance of the coatings and substrate were specified in dry, serum (0.9 wt.% NaCl solution) and simulated body fluid (SBF) -according to recipe of Tas [70]- environment under testing load of 1 N for all cases by using of Tribotech^{TM} reciprocating wear tester. For dry and serum environments, temperature fixed at room temperature. In contrary, testing in SBF environment temperature fixed at 36.5 ^oC to simulate human body conditions. During wear test, Al_2O_3 ball with a diameter of 6 mm was used as a counter body. Moreover, sliding velocity, sliding stroke and total sliding length were fixed as 10mm/s, 5mm and 25m, respectively. Coefficient of friction was recorded by wear tester throughout the testing period. After the test, wear scars of samples and worn surface of counterbody (Al_2O_3 ball) were investigated by optical microscopy. Additionally, Dektak 6M 2-D profiolometer was enrolled to evaluate worn area of the coating and substrate.

3.4 Biological Test

In this section, experimental procedure of biological test for copper and aluminium containing coatings will be briefly explained.

3.4.1 In vitro bioactivity test

Schematic representation of in vitro bioactivity test of coating that, executed after thermal oxidation in simulated body fluid can be seen in Figure 3.2.

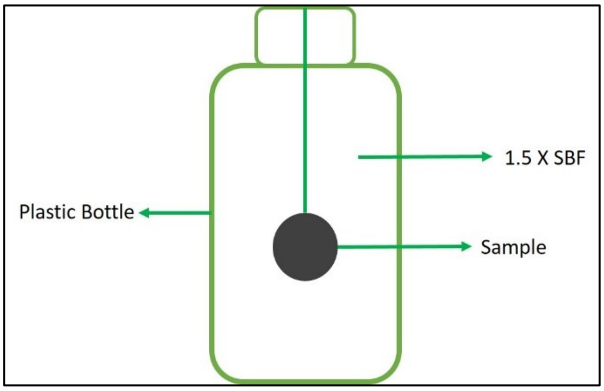

Figure 3.2: Schematic projection of it vitro bioactivity test

Contents of prepared simulated body fluid according to Tas' recipe [70] can be seen in Table 3.3. Additionally, for this biological test 1.5X SBF was chosen due to simulate test in higher speed. After in vitro bioactivity test the samples taken out from the SBF and their surfaces were examined with SEM.

Table 3.3: Content of simulated body fluid

ION	Na^+	K^+	Mg^{2+}	Ca^{2+}	HPO_4^{2-}	HCO_3^-	Cl^-	SO_4^{2-}	Buffering Agent
nM	142	5	1.5	2.5	1	27	125	0.5	Iris

4. RESULT & DISCUSSION

4.1 Structural Characterization of Cu Containing Coatings

In section 4.1, results of the microscopic investigations, x-ray diffraction analysis and roughness measurements for the copper containing will be clarified.

4.1.1 Microstructural characterization of coatings

As briefly explained above, copper powders with different ratios (5 wt. % Cu – 3 wt. %Cu and 1.5 wt. %Cu) and iron oxide powder in magnetite form at fixed ratio of 3 wt. % were mixed with titanium due to high plastic deformability and positive biological effects such as antibacterial behaviour and increased bioactivity. In the scope of the study, content of the copper in feedstock aimed to be decreased, due to concerns about the well-known toxic effect of copper oxide compound without sacrificing continuity on structure. For that reason, initially microstructure of copper containing coatings were investigated and optical micrographs before and after thermal oxidation were given in Figure 4.1. It is clearly seen that, titanium based coating with addition of 5 wt.% Cu and 3 wt.% Fe_3O_4 successfully formed and oxidized on the surface of Co-Cr substrate without any discontinuity (such as, high porosity or gap on interface). On the other hand, decrement on the copper amount inside the powder mixture directly affect the microstructures result in discontinuities arisen. In addition, efficiency of CS process decreased respect to copper amount inside powder mixture and thickness of coatings reduced to 250 μm from 450 μm. Therefore, 5 wt. % Cu-3 wt.% Fe_3O_4- 92 wt.% Ti feedstock composition was used for coating processes. Thus, from now, other characterization and biological tests will be executed for coating which processed with this composition.

Cross sectional SEM micrographs of Cu containing coatings after thermal oxidation are given in Figure 4.2. It is clearly seen that, during thermal oxidation about 2-3 μm thick oxide layer successfully formed on the outermost surface and no discontinuity at the coating/substrate interface was observed. Additionally, cracking of brittle phases during metallographic sample preparations due to extreme mechanic effects can be the main reason of discontinuities and spallation on oxide layer. Moreover, existence of dark gray solid solution phases around titanium particles on the interface of coating and substrate may show diffusion of oxygen throughout the coating thickness.

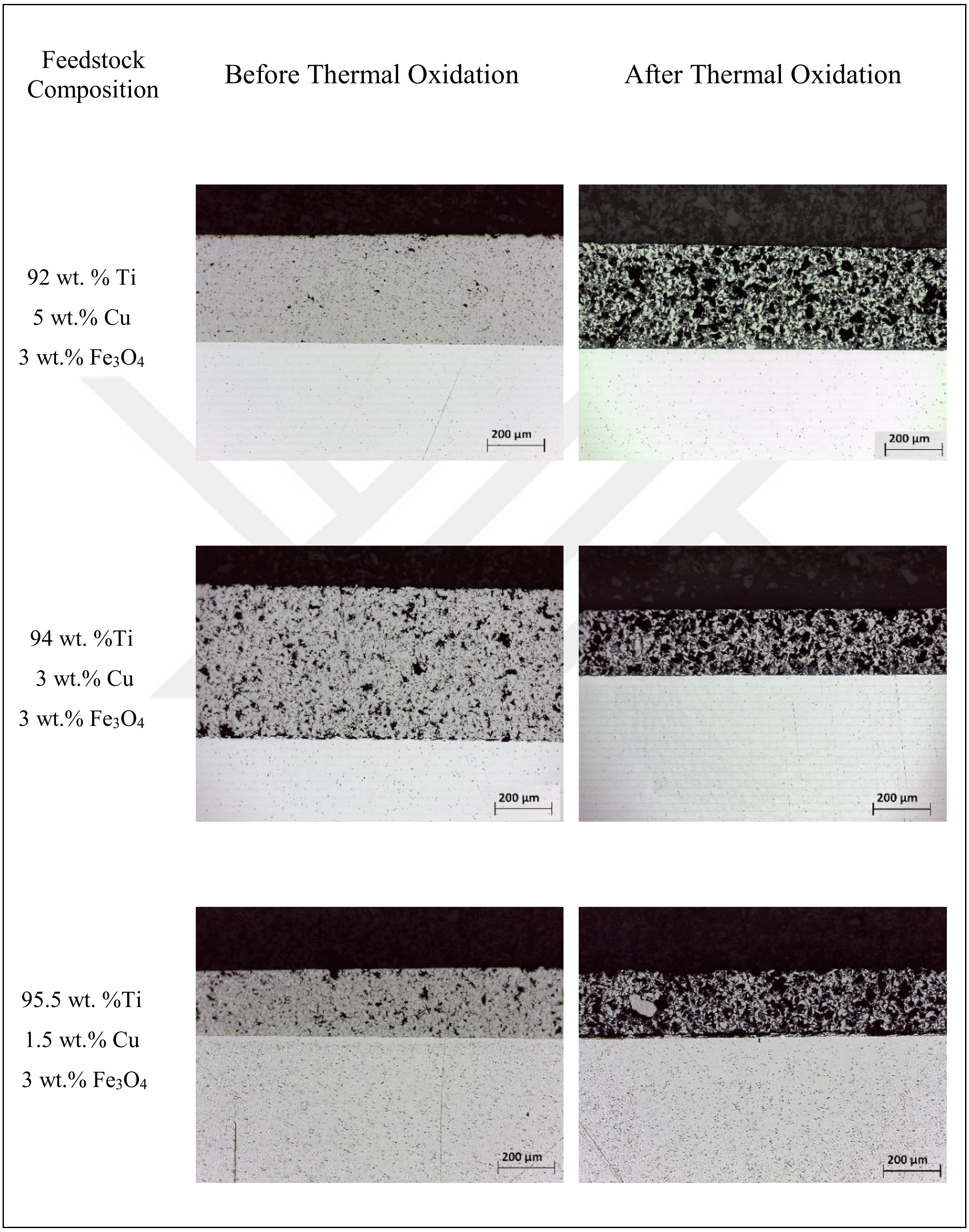

Figure 4.1: Optical micrographs of Cu containing coatings before and after thermal oxidation

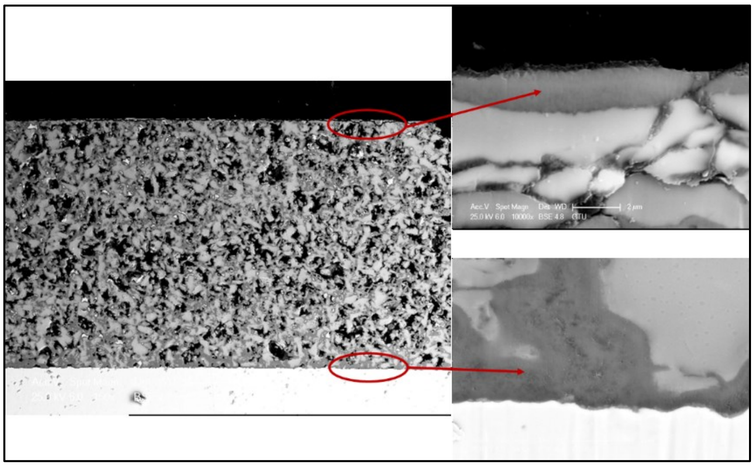

Figure 4.2: SEM micrographs of coating deposited by 5 wt.% Cu containing feedstock after thermal oxidation

Dark regions in Figure 4.2 arouse a thought of high porosity formation during thermal oxidation. To be sure, if it is porosity or another phase, SEM was enrolled in both backscatter (BSE) and secondary (SE) electron mode and micrographs of Cu containing coating are depicted in Figure 4.3. SEM image taken in SE mode clearly shows evidence of another phase in dark regions and low amount of porosity in microstructure (Figure 4.3-b).

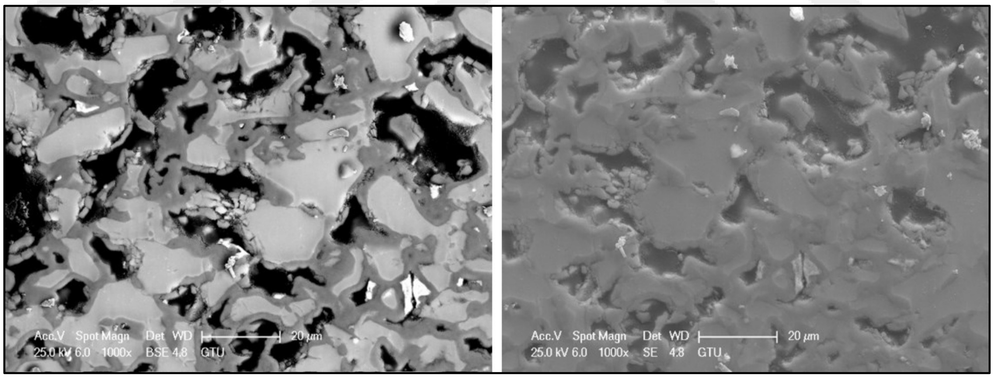

(a) (b)

Figure 4.3: BSE (a) and SE (b) SEM micrographs of coating deposited by 5 wt.% Cu containing feedstock after thermal oxidation

After thermal oxidation, EDX area analyses were carried out from five different regions to evaluate compositional differences, which seem as different color in SEM images. Then, atomic percentages are given in Figure 4.4 confirming the percentage of existing component in the coating. When the atomic ratios of gray, dark gray and light regions are evaluated; in gray regions (region 1) presence of titanium and oxygen, in/or around light regions (region 2 and 3) presence of copper, in dark gray regions presence of titanium and oxygen with higher amount of oxygen were detected. This determinations show during thermal oxidation oxygen atoms may diffuse in to the titanium particle and this diffusion may lead the formation of solid solution regions in dark gray color. In addition, brittle iron oxide particles settled to the titanium and copper particle boundaries due to probable fragmentations of during cold spraying process. This prediction may explain very low amount of iron presence in region 5 and 6 in Figure 4.4.

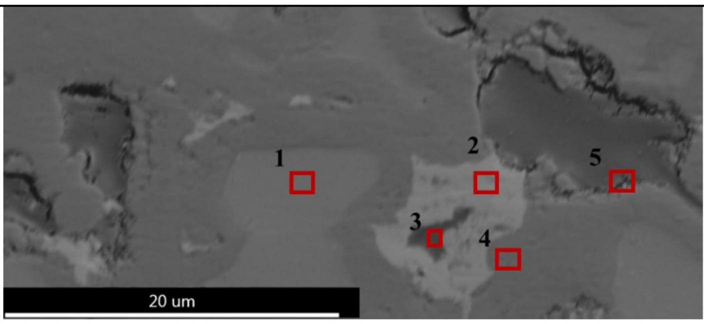

Element At %	1	2	3	4	5
Titanium	73.3	4.7	9.8	35.3	17.9
Copper	0.2	87.3	76.7	4.8	8.6
Iron	0.7	0.6	1.5	5.4	5.3
Oxygen	25.8	7.4	12	54.5	68.2

Figure 4.4: EDX carried out regions and atomic percentage results of the oxidized coating deposited by 5 wt.% Cu containing feedstock after thermal oxidation

SEM EDX area analyses were performed from the cross-section of the oxide layer and the results are given with analyzed regions and atomic proportions in Figure 4.5. Atomic percentages shows that, titanium based oxide layer successfully formed. In addition, copper and low amount of iron probably in magnetite form preserve the existence like beneath the oxide layer.

SEM-EDX line scans of different regions were carried out from the polished cross-section of coating and scan region is shown in Figure 4.6, revealing that, atomic amount of titanium decrease and oxygen increase in dark gray region around copper particle. In addition, inside the copper particle presence of any other element could not detected.

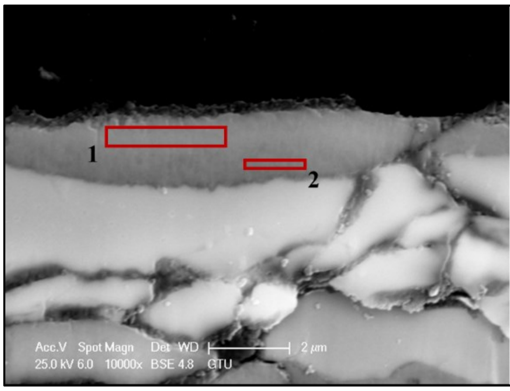

Element At. %	1	2
Titanium	36.9	35.3
Copper	0.6	4.8
Iron	1.4	5.4
Oxygen	61.1	54.5

Figure 4.5: Carried out EDX area regions and atomic percentage results of the oxide layer on coating deposited by 5 wt.% Cu containing feedstock

In titanium oxygen and copper ternary system, reaction between titanium and oxygen may not lead the oxidation of copper. Therefore, dark gray solid solution phases forms around copper particles in entire microstructure. This phenomenon, can be explain with higher affinity of titanium to oxygen. Additionally, line scan analysis results support the projected findings in EDX.

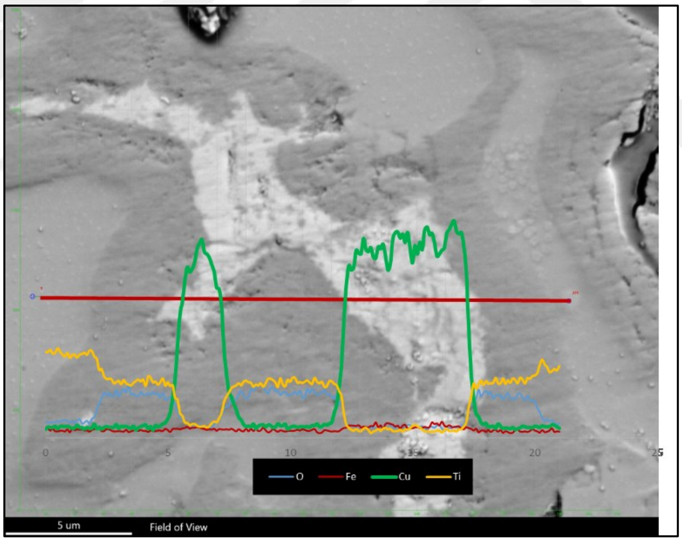

Figure 4.6: SEM-EDX line scans of the coating deposited by 5 wt.% Cu containing feedstock after thermal oxidation

4.1.2 X-ray diffraction (XRD) analysis

XRD patterns of the coatings before and after thermal oxidation were given in Figure 4.7. Before thermal oxidation only α-titanium and copper peaks were detected while no presence of iron oxide peaks due to deposited amount less than 3 wt.%. This result directly match with contains of the feedstock and showed that, during cold spraying process no chemical reaction took place between deposited materials. Otherwise, after thermal oxidation, only peaks of titanium and titanium dioxide in the form of rutile was appeared in the XRD patterns. Additionally, titanium peaks preserved the existence in the oxidised coatings due the penetration of X-rays beneath the oxide layer during analyses. Moreover, shifting of α-titanium peaks to the left around 1^0 after oxidation was detected and this condition showed that titanium phase beneath the oxide layer is in the form of solid solution due to the oxygen penetration.

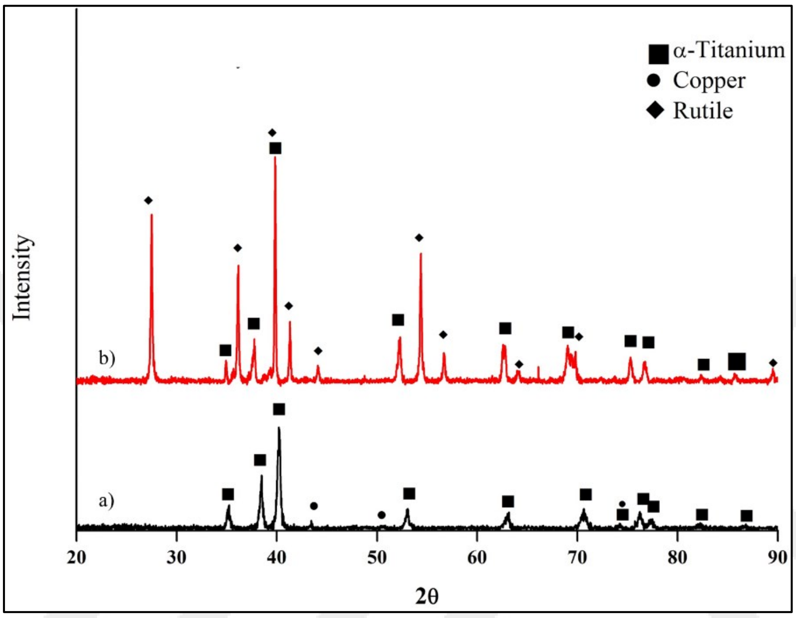

Figure 4.7: XRD patterns of the coating deposited by 5 wt.% Cu containing feedstock (a) before and (b) after thermal oxidation

4.1.3 Surface Roughness Measurement

Before and after thermal oxidation surface roughness of coating deposited by 5 wt. % Cu containing feedstock measured. By the effect of thermal oxidation average surface roughness (Ra) of the coating increased from 0.111 to 0.629 µm. It is known from the literature this roughening is the characteristic result of thermal oxidation of titanium [7]. Also it should be noted that, this result is favorable for the aim of study cause, rough surfaces of metallic bio materials show better interaction with surrounding tissue with more bioactive behavior.

4.2 Mechanical Properties of Cu Containing Coatings

In this section, mechanical properties including hardness measurements and tribology tests of the copper containing will be explained.

4.2.1 Hardness measurement

Hardness of the coating was determined before and after thermal oxidation from the crossection and listed in Table 4.1. This dramatic increment from 68±4 to 533.5±69 $HV_{0.025}$ in while increasing of porosity can be mainly related with the diffusion of the oxygen into the titanium and formed the solute solution in the coating according to phase diagram of titanium-oxygen [59]. Moreover, surface hardness was measured as 879,5 ± 167.9 HV via micro-nano hardness tester.

Table 4.1 : Crossectional and surface hardness of oxidized coating deposited 5 wt. % Cu containing feedstock

Before Thermal Oxidation	After Thermal Oxidation	
Crossectional	Crossectional	Surface
68.7 ± 4.33 $HV_{0.025}$	533.5± 69.6 $HV_{0.025}$	879,5 ± 167.9 HV

4.2.2 Tribological test

Tribological performance of Co-Cr susbtrate and the oxidized coating deposited by 5 wt. % Cu containing feedstock determined in dry, serum and SBF environment. For all the cases, friction coefficient increases up to the specific level and become stable running in period. For that reason steady state friction coefficient values obtained from friction coefficient curves in Figure A.1 and results are given in Table 4.2. Furthermore, while Co-Cr substrate shows the similar chracteristics in any environment, friction coefficient of coating in dry testing condition is lower than that of Co-Cr substrate in contrast to the serum and SBF conditions. This result could be explained with the OM images of worn surfaces. Whereas none effect of wear could be detected from the worn surface of coating, clear wear scar obtained from the surface of the Co-Cr alloy in contrary (Figure 4.8). In our best knowledge, during dry sliding wear testing of coating, between the counter body material (Al_2O_3 ball) and the oxide layer on the outermost surface lubricant effect could be observed because of ceramic-ceramic interaction.

Otherwise, tribological performance of oxidized coating was concern in serum and SBF environment relatively higher friction coefficient and more apparent impressions on worn surface were spotted in Table 4.2 and Figure 4.8 respectively.

Table 4.2: Steady state friction coefficients of substrate and coating deposited by 5 wt. % Cu containing feedstock

Testing Environment	Steady State Friction Coefficients of Substrate	Steady State Friction Coefficients of Coating
Dry	0.29	0.18
Serum	0.26	0.51
SBF	0.26	0.37

Serum and SBF are corrosive isotonic salt solutions because of the corrosive ions eg. Cl^- and $H_2PO_4^-$ etc and easly react with titanium oxide. Moreover, the wear testing load of 1N creates 840 MPa Hertzian contact pressure on the contact surface of the coating. Combinations of these two situation induce an increment on the friction coefficients.[71, 72].

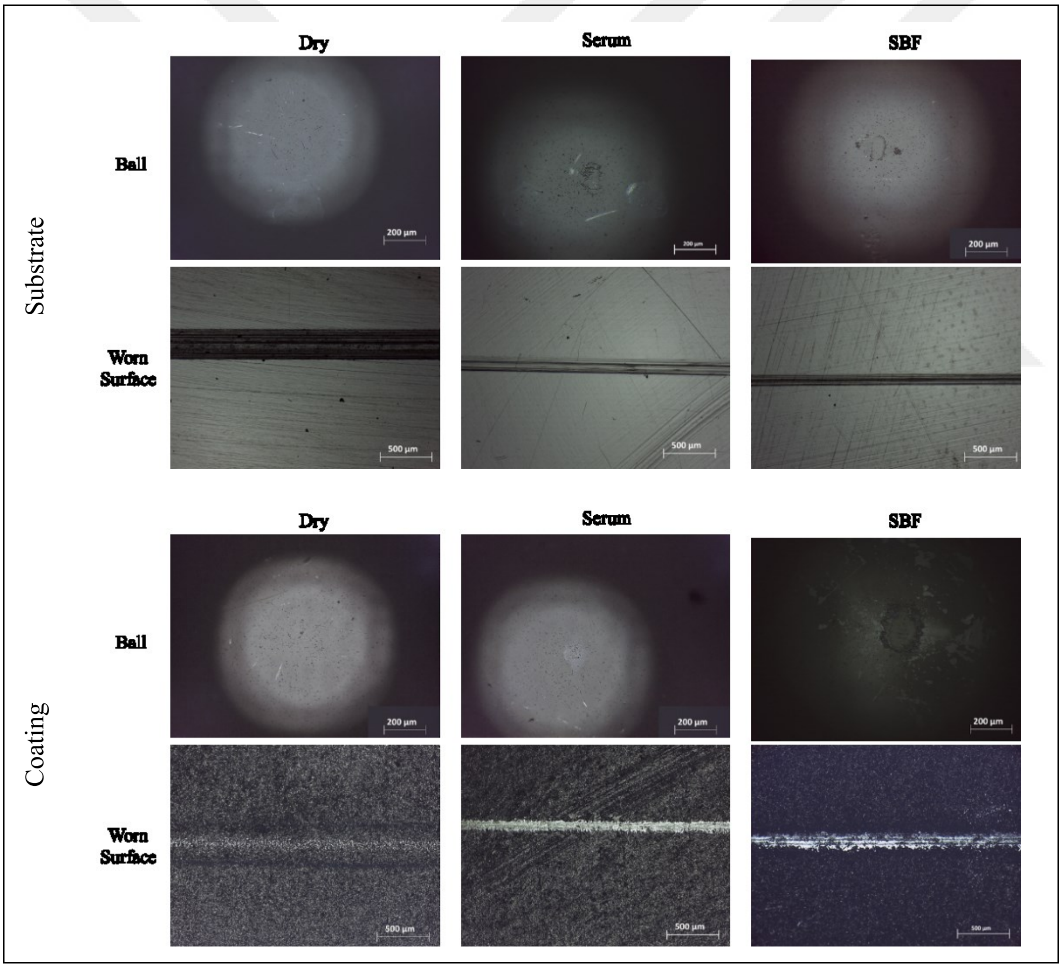

Figure 4.8: Worn surface of substrate, coating deposited by 5 wt. % Cu containing feedstock and alumina balls respect to testing environment

Wear scar appearances on the surface of alumina balls for Co-Cr substrate and coating are showing parallelism with OM images of wear tracks; for the balls, which used for during testing of substrate have more significant wear scars on the surface compare to the balls used for coatings' wear tests in any environment.

4.3 Biological Test of Cu Containing Coatings

In this section, result of the biological test for copper containing coatings will be explained briefly.

4.3.1 In vitro bioactivity test

After in vitro bioactivity test, the surface of copper containing coating, showed the formation of a new structure in the same morphology with Hydroxyapatite [8]. The uniform and gathered sphere like particles has covered the entire specimen surface after immersion in SBF for 1 week (Figure 4.9). Moreover, when the immersion time increased to 4 weeks, the acceleration in the growth of spherical particles on the oxide surface can be seen clearly.

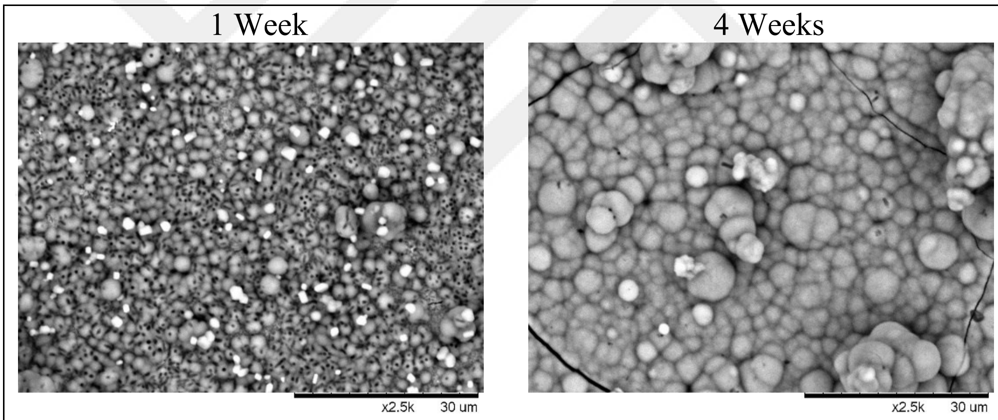

Figure 4.9: SEM micrographs of the Cu containing coatings after 1 and 4 weeks in vitro bioactivity test

4.4 Structural Characterization of Al Containing Coatings

In section 4.4, results of the microscopic investigations, x-ray diffraction analysis and roughness measurements for the aluminum containing will be clarified.

4.4.1 Cross-sectional microstructure characterization of coatings

In the second part of the study, aluminium and titanium powders were mixed at constant percentage of aluminum (8 wt.% Al) to improve efficiency of cold spraying process. Moreover, 5 wt. % zinc, and/or 3 wt. % iron oxide powders were added to feedstock to improve biological properties of coating (list of aluminium contaning feedstock which are deposited to the Co-Cr substrate can be found in Table 3.2). While, zinc was chosen for potential antibacterial property, iron oxide was chosen for bioactive effect as discussed in section 1. OM images of these coatings before and after thermal oxidation are presented in Figure 4.10.

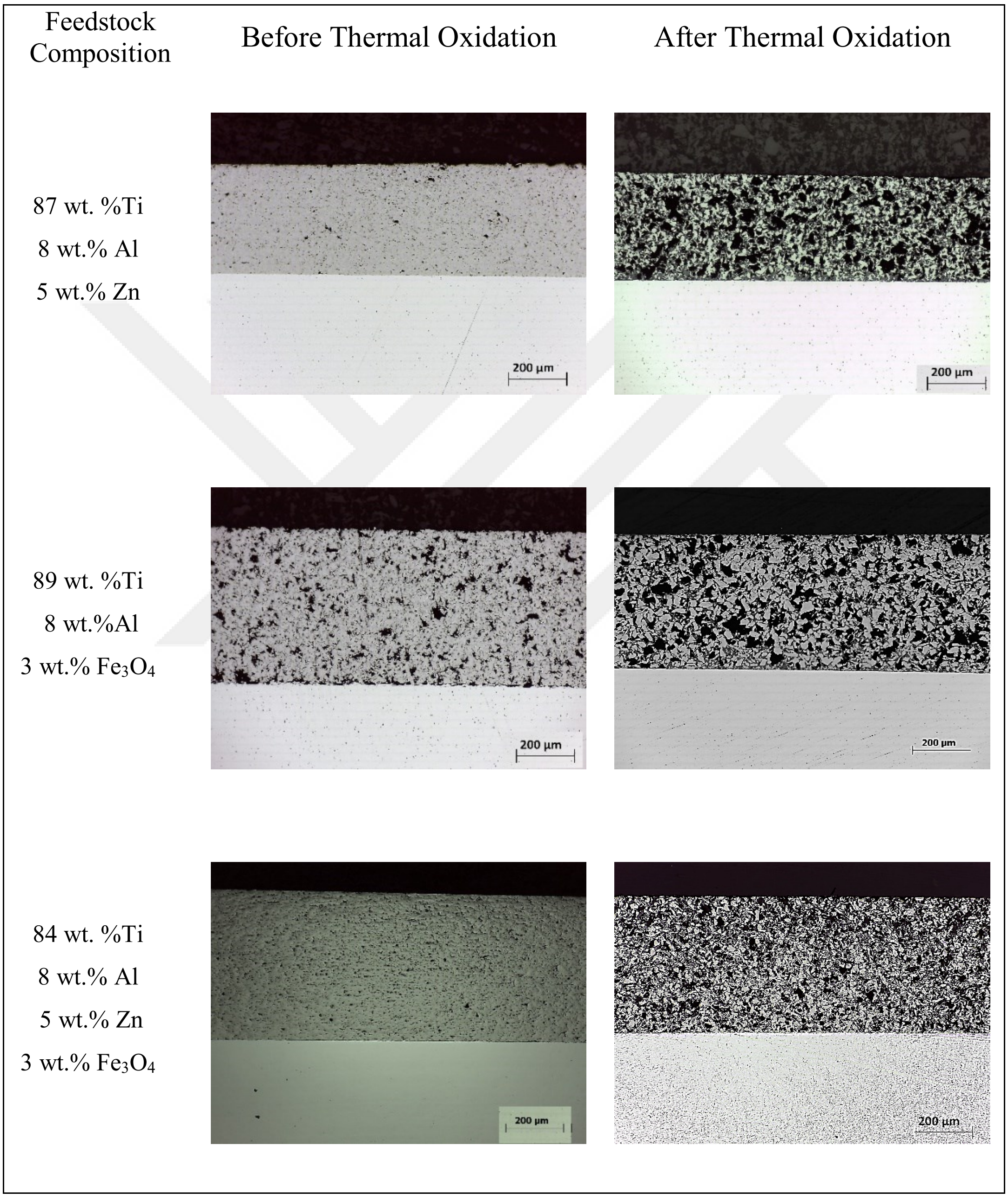

Figure 4.10: Optical micrographs of Al containing coatings before and after thermal oxidation

In all cases, feedstock were deposited with high efficiency and around 450-500 µm thick coating formed on the surface of F75 grade Co-Cr alloy. Moreover, it is not possible to talk about the effect of other additives in to titanium-aluminum powders mixture to the efficiency of cold spray process. Images taken before the thermal oxidation refer functional coating thickness without any dead zone on the outermost section. Moreover, the samples, which would expose the thermal oxidation, thickness of coatings, were reduced with abrasive papers in metallographic stages to avoid possible thermal expansion fails.

Feedstock Composition	Crossestional SEM micrograph
87 wt. %Ti 8 wt.% Al 5 wt.% Zn	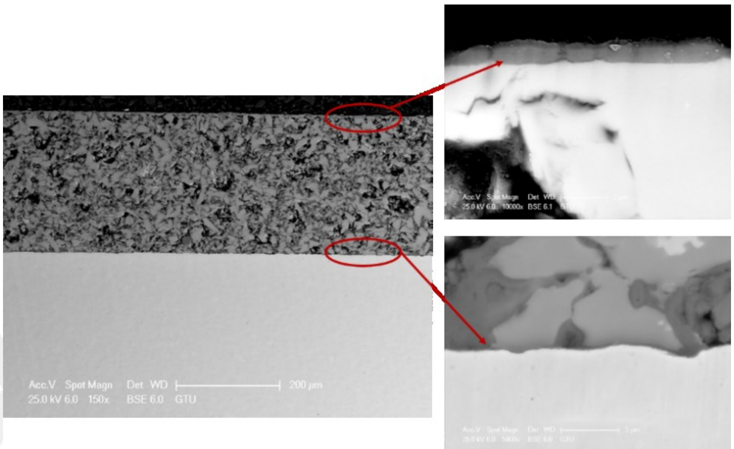
89 wt. %Ti 8 wt.%Al 3 wt.% Fe_3O_4	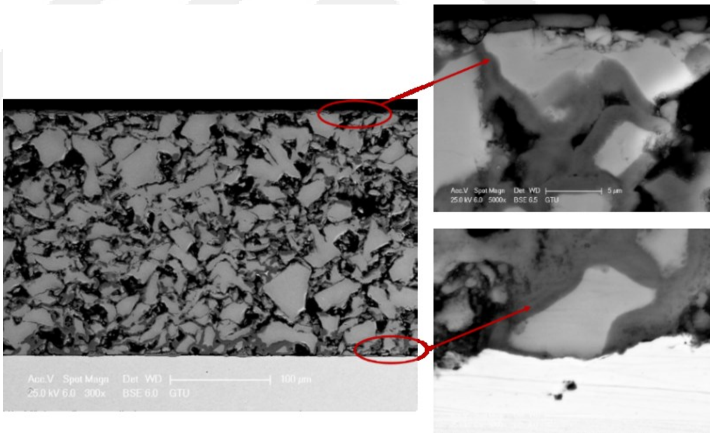
84 wt. %Ti 8 wt.% Al 5 wt.% Zn 3 wt.% Fe_3O_4	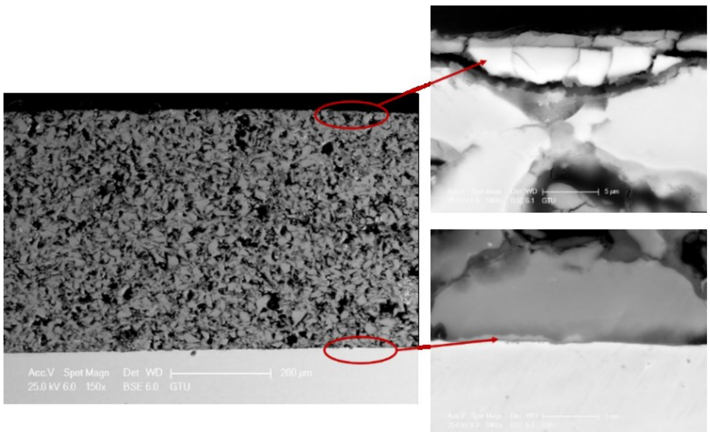

Figure 4.11: Crossestional SEM micrographs of Al containing coatings after thermal oxidation

Cross sectional SEM micrographs of Al containing coating after thermal oxidation are given in Figure 4.11. For all the compositions, while no discontinuity on the interface of coating and the substrate surface could be pointed out, the thickness of oxide layer (2-3 µm) on the outermost surface remained same.

Nevertheless, high mechanical effect during metallographic stages can cause crack formation on oxide layers. Like as copper containing coating, high penetration and diffusion of oxygen in to the deep of the coating may be the reason of dark gray regions on interface and around the titanium particles.

High magnification SEM images of Al containing coatings were taken in BSE and SE mode and illustrated in Figure 4.12. Four different phase stood out from the examinations of BSE images of micro structures; dark, dark gray, gray in all coatings and light in Zn containing coatings. These differences in color contrast directly related with the density of different phases, for instance oxide phases seem darker due to lower density. In other respect, SE SEM images reveal another phase in dark regions and very low amount of porosity even after thermal oxidation.

Elemental distributions in different regions determined by EDX area analysis from the polished cross-section of Al containing coating. Selected regions and elemental atomic percentages are given in Figure 4.12 for each composition. The first appearance from the EDX analyses is the high amount of zinc inside and/or around the titanium particles (Figure 4.13-regions 6, 7,15,16,18 and 19). This demonstrate of zinc diffusion in to titanium particles during thermal oxidation. Under the light of this observation, when the zinc-titanium binary phase diagram is studied, there is no solubility of zinc inside the titanium. Therefore, these whitish regions may refer the $TiZn_2$ intermetallic compound.

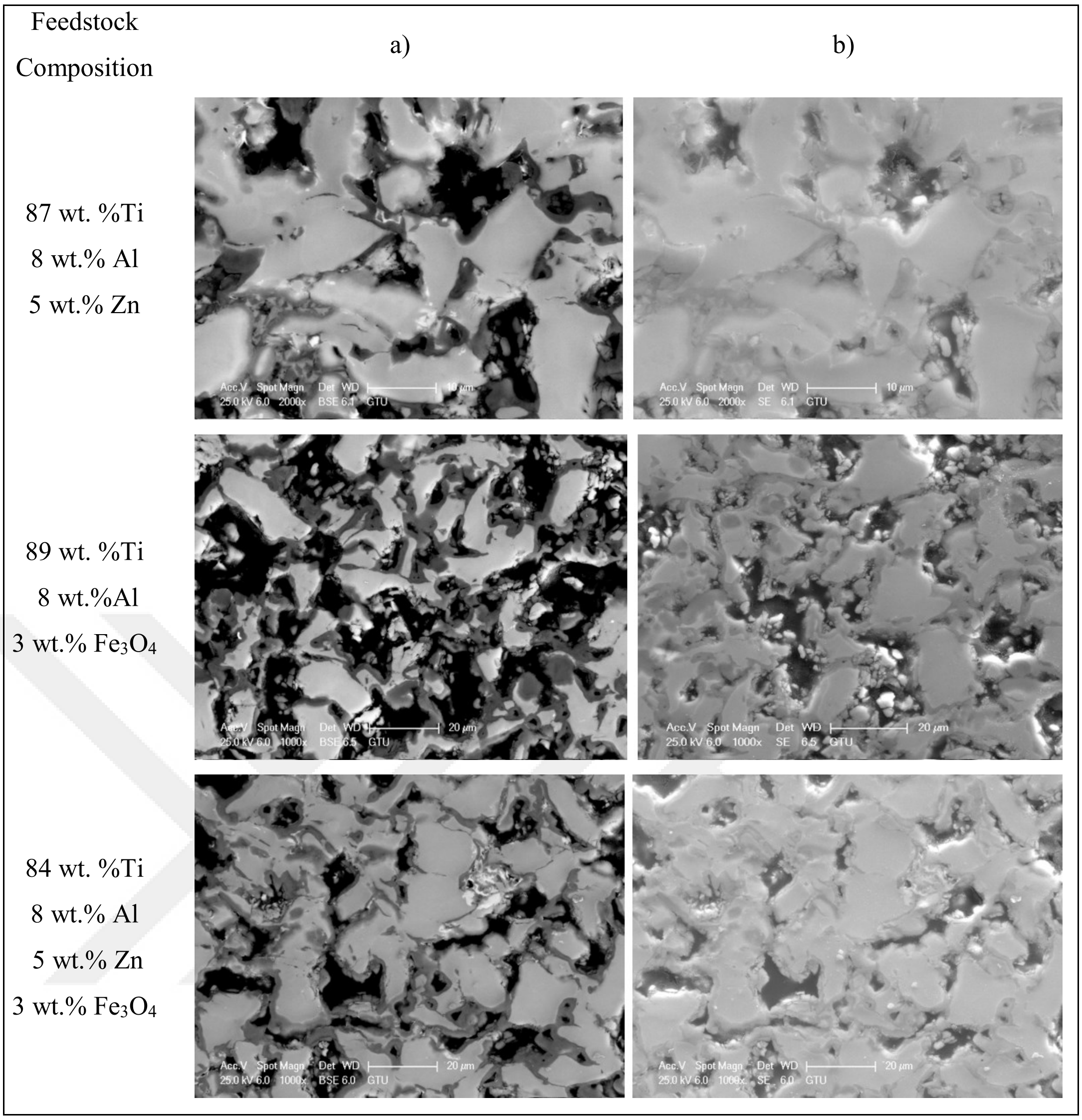

Figure 4.12: Detailed BSE a) and SE b) mode SEM micrographs of Al containing coatings after thermal oxidation

Moreover, oxygen penetration and diffusion around the titanium particles and formed the titanium oxygen solid solution region in dark gray color (Figure 4.13 region 5, 12 and 14). Additionally, different phases were appeared on interface of aluminum titanium particles due to diffusion of aluminum inside the titanium (the regions 1, 2, 8, 9 and 10). In that respect, these regions may refer titanium-aluminum intermetallic compounds such as Ti_3Al, TiAl, $TiAl_3$ according to titanium aluminum phase diagram. Furthermore, similar results were caught for iron oxide, again due to probable fragmentations of brittle iron oxide particle during cold spraying process cause settlement of these particles in to the interface of titanium and other particles such as regions 17 and 22.

Feedstock Composition	Selected Regions and Atomic Percentages

87 wt. %Ti
8 wt.% Al
5 wt.% Zn

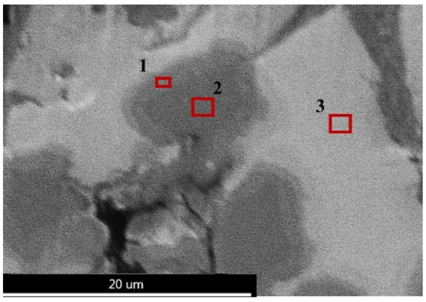

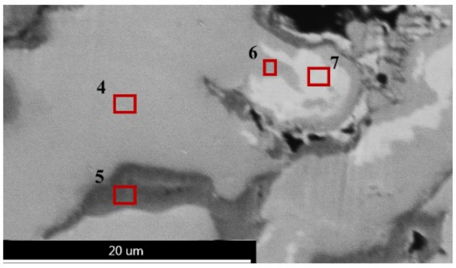

Element At. %	1	2	3	4	5	6	7
Titanium	63.7	24.7	78	79.4	38.7	62.5	62.1
Aluminum	16.7	70.5	0.29	0.16	0.02	5.6	2.3
Zinc	0.56	0.01	0.26	0.28	0.04	24.8	27.5
Oxygen	18.9	4.8	21.4	19.8	61.2	7.4	7.9

89 wt. %Ti
8 wt.%Al
3 wt.% Fe_3O_4

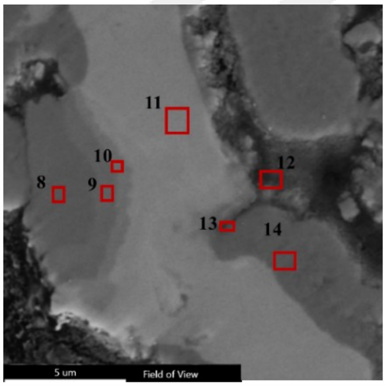

Element At. %	8	9	10	11	12	13	14
Titanium	24.5	23.6	67.6	71.4	32.2	45.3	33.4
Aluminum	73.1	69.4	19.4	0.2	5	0.9	0.2
Iron	0	0.1	0.5	0.1	2.5	1.1	0.3
Oxygen	2.3	6.9	12.5	28.3	60.3	52.7	66.1

84 wt. %Ti
8 wt.% Al
5 wt.% Zn
3 wt.% Fe_3O_4

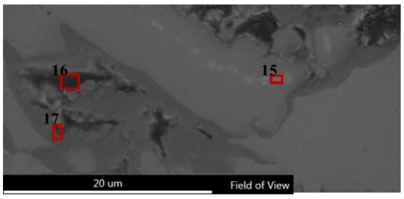

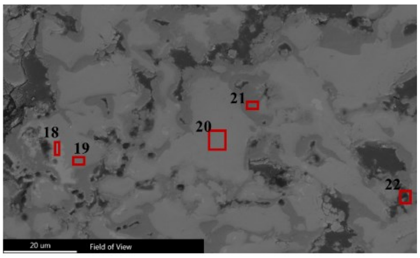

Element At. %	15	16	17	18	19	20	21	22
Titanium	61.1	57.2	6.8	8.5	59.7	75.3	60.7	14.8
Aluminum	2.1	4.6	0.8	5.1	0.5	0.4	0.3	28.7
Zinc	31	25.5	3.6	38.8	33.1	0.4	0.5	9.5
Iron	0.1	0.2	20	0	0.1	0.7	0.2	18.1
Oxygen	5.3	12.5	68.2	47.6	6.6	25.2	38.3	29

Figure 4.13: Cross-sectional EDX analyses of Al containing coatings after thermal oxidation

Feedstock Composition	Selected Regions and Atomic Percentages

87 wt. %Ti
8 wt.% Al
5 wt.% Zn

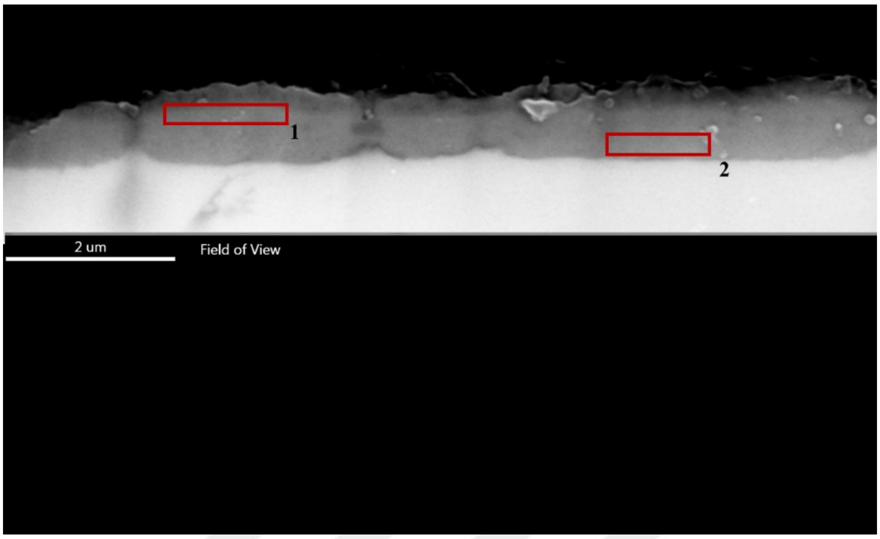

89 wt. %Ti
8 wt.%Al
3 wt.% Fe_3O_4

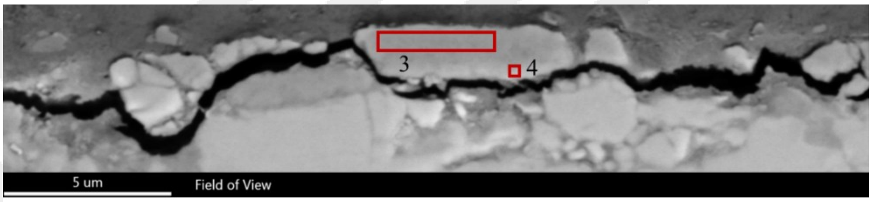

Element At. %	3	4
Titanium	32.3	33.2
Aluminum	0.4	0.3
Iron	0.6	0.6
Oxygen	66.7	65.9

84 wt. %Ti
8 wt.% Al
5 wt.% Zn
3 wt.% Fe_3O_4

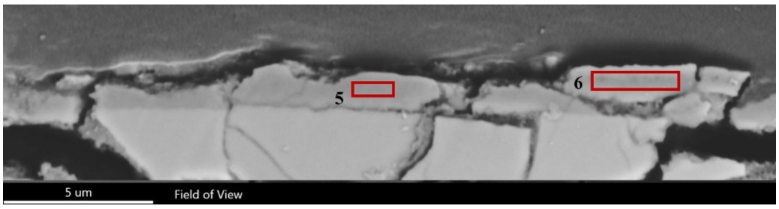

Element At. %	5	6
Titanium	30.5	34.2
Aluminum	0.3	0.3
Zinc	0.5	0.3
Iron	1.1	0.5
Oxygen	67.6	64.7

Figure 4.14: Carried out EDX area regions and atomic percentage results of the oxide layer on Al containing coatings

Feedstock Composition	Selected Line
87 wt. %Ti 8 wt.% Al 5 wt.% Zn	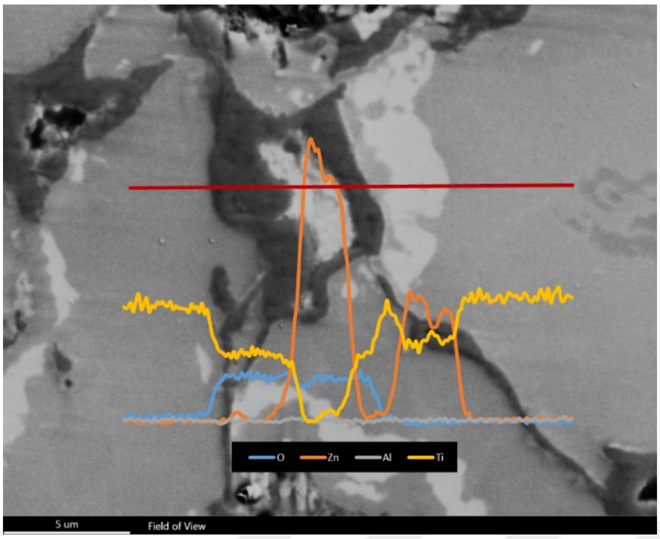
89 wt. %Ti 8 wt.%Al 3 wt.% Fe_3O_4	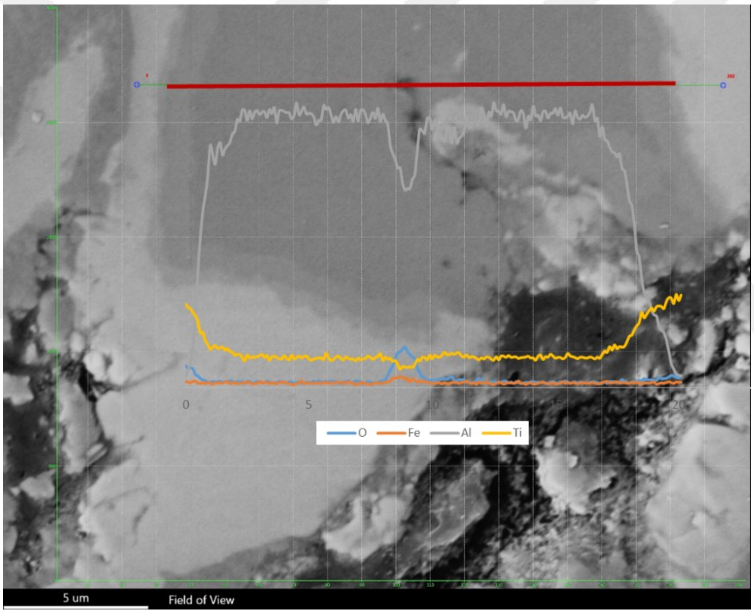
84 wt. %Ti 8 wt.%Al 5 wt. % Zn 3 wt.% Fe_3O_4	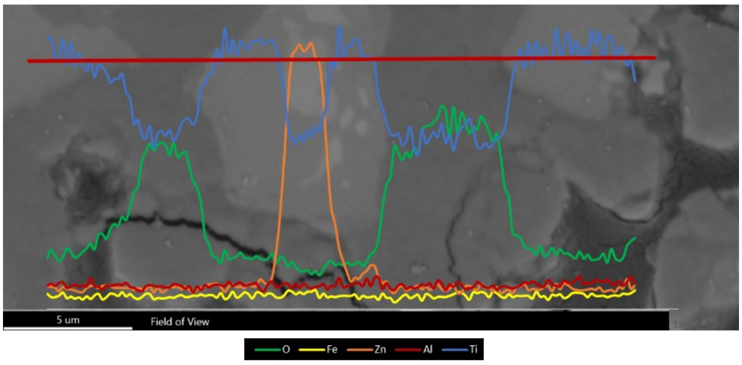

Figure 4.15: EDX line scans of Al containing coatings after thermal oxidation

In order to evaluate elemental content of oxide layers, EDX analyses also performed from the polished cross-section of oxides on Al containing coatings and result are presented in Figure 4.14 with selected regions and atomic ratios. For all the selected regions in coatings, around ½ atomic ratio of titanium to oxygen were determined and this result may thought formation of TiO_2 compound on the outermost surface of coating. Additionally, zinc and iron oxide additives are continuing to existence in oxide layer as well.

EDX line scan analyses performed on different region of polished cross-section of coatings and plots of the relative elemental concentration for each element are presented in Figure 4.15. The plots verify the estimations that are done respect to the result in EDX area analysis and clarify zinc diffusion in to titanium particle. Additionally, around the titanium particles dark gray regions refer possible solid solution phases like depicted in EDX area analysis. Moreover, plot of the coating deposited by feedstock 89 wt. %Ti – 8 wt. %Al – 3 wt.%Fe_3O_4 proves the estimation about settlement place of iron oxides and diffusion of aluminum in to the titanium particle.

4.4.2 X-ray diffraction (XRD) analysis

XRD patterns of the aluminium containing coatings before and after thermal oxidation process are given in Figure 4.16. For all the coating, before thermal oxidation only the peaks of feedstock content were detected on the XRD pattern (except iron oxide). Otherwise, after 60 hour at a temperature of 600 ◦C thermal oxidation, peaks of aluminium oxide and α-titanium beside the titanium di-oxide in the form of rutile were appeared in the XRD patterns. No peaks of iron oxide for all the coatings before and after thermal oxidation may be related with presence of this additive inside the coating composition less than detachable amount of 3 wt. %. It can be concluded from the XRD analyses, during the thermal oxidation process oxide layer consist of titanium di-oxide and aluminium oxide formed as the results of reaction between titanium and aluminium with oxygen individually. Furthermore, presence of the α-titanium in the XRD patterns after oxidation is related to the penetration of X-rays beneath the oxide layer during analyses.

4.4.3 Surface Roughness Measurement

Surface roughness of the Al containing coating was examined before and after thermal oxidation. The results in Table 4.3 showed that the roughness increase by a factor of 6 as natural outcome of the thermal oxidation [7]. This increment in roughness provide the bio-activity of the coating via increasing the interaction of the surface and the surrounding tissues.

Table 4.3: Surface roughness values of Al containing coatings

	Before Thermal Oxidation		After Thermal Oxidation	
Feedstock Composition (Wt. %)	Ra	Rz	Ra	Rz
8%Al + 5% Zn + 87% Ti	0.107 ± 0.01	0.687± 0.07	0.631± 0.01	3.811± 0.04
8% Al + 3% Fe_3O_4 + 89% Ti	0.119± 0.02	0.607± 0.06	0.542± 0.015	2.521± 0.08
8%Al + 5% Zn + 3% Fe_3O_4 + 84% Ti	0.121± 0.01	0.557± 0.07	0.621± 0.02	3.205± 0.05

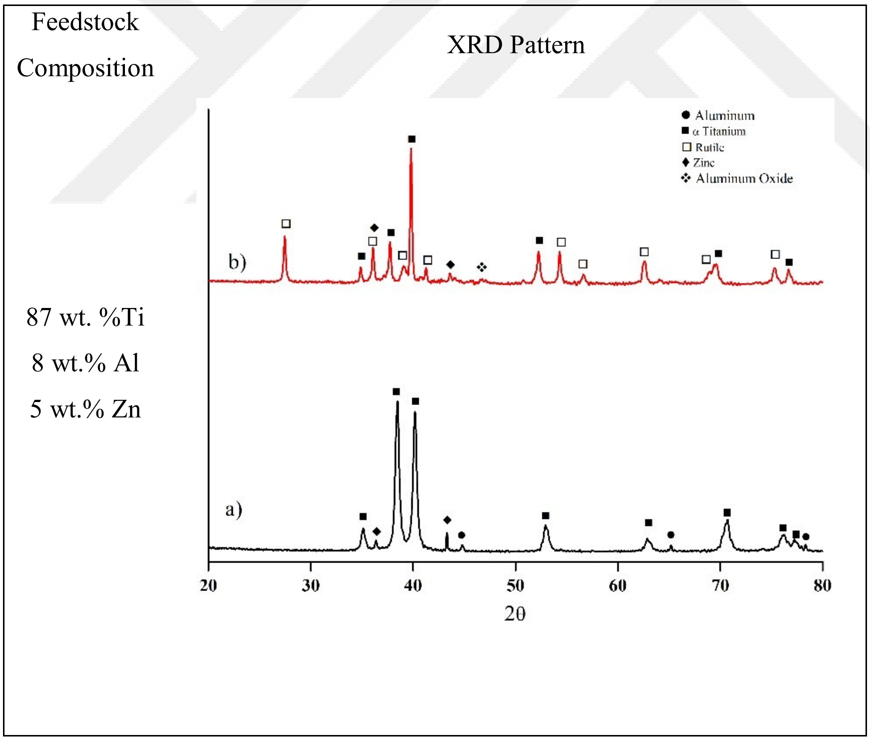

Figure 4.16: XRD patterns of Al containing coatings a) before and b) after thermal oxidation according to feedstock compostion

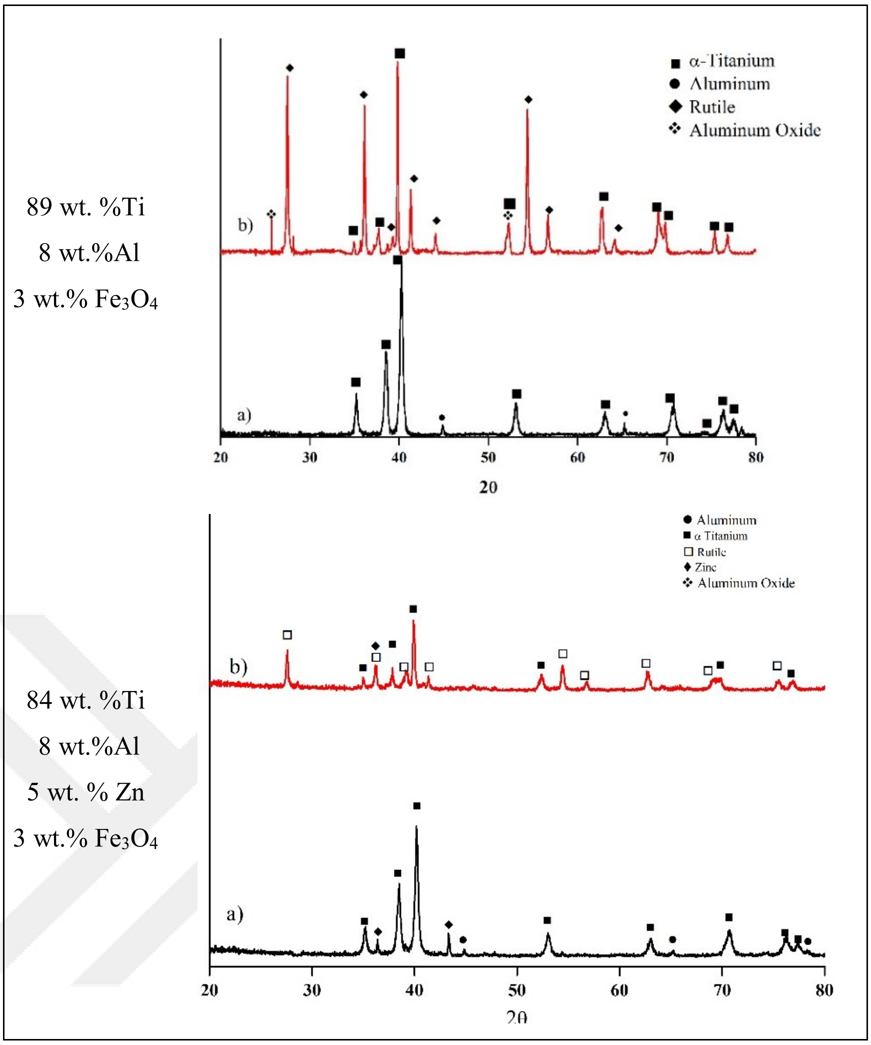

Figure 4. 16 (Cont.): XRD patterns of Al containing coatings a) before and b) after thermal oxidation according to feedstock compostion

4.5 Mechanical Properties of Al Containing Coatings

In this section, mechanical properties including hardness measurements and tribology tests of the copper containing will be explained.

4.5.1 Hardness measurement

Cross-sectional hardness of the coating was measured before and after thermal oxidation with Vickers indenter and values are given in Table 4.4.

Table 4.4: Crossectional and surface hardness of Al containing coatings.

	Before Thermal Oxidation	After Thermal Oxidation	
Feedstock Composition (Wt. %)	Crosssectional $HV_{0.025}$	Crosssectional $HV_{0.025}$	Surface HV
8%Al + 5% Zn + 87% Ti	79.5 ± 23.1	449.4 ± 54.1	943.6 ± 158.5
8% Al + 3% Fe_3O_4 + 89% Ti	67.4± 5.1	414.1± 61.1	857.7 ± 201.9
8%Al + 5% Zn + 3% Fe_3O_4 + 84% Ti	111.2±13.5	473.4±52.9	851.1 ± 196.6

Around five times increment in hardness was observed for all composition due to penetration of oxygen in to the coatings and solid solutions and/or intermetallic compound formed as an expected because of chemical reactions during thermal oxidation. Moreover, hardness of the oxide layers measured around 900 HV for all the coatings. It can be concluded as, it is not possible to mention from the effect of different additives on cross-sectional and surface hardness.

4.5.2 Tribological test

Tribological performance of Al containing coating determined in dry, serum and SBF environment. For all the cases, friction coefficient increases up to the specific level and become stable running in period. Hence, steady state friction coefficients were obtained from friction coefficient curves in Figure A.1 and results are listed in Table 4.5.

Table 4.5 Steady state friction coefficients of Al containing coatings

	Testing Environment		
Feedstock Composition (Wt. %)	Dry	Serum	SBF
8%Al + 5% Zn + 87% Ti	0.08	0.38	0.26
8% Al + 3% Fe_3O_4 + 89% Ti	0.23	0.36	0.28
8%Al + 5% Zn + 3% Fe_3O_4 + 84% Ti	0.09	0.4	0.27

When the dry sliding conditions are concern, Zn containing coatings exhibit lower friction coefficients. Lubricant effect of metallic zinc or/and zinc-titanium intermetallic compound in the oxide surface may cause this low friction coefficient behavior in dry sliding conditions. Additionally, all the coatings revealed similar friction coefficient characteristic with Cu containing coating due to explained behavior of titanium oxide in serum and SBF testing environment. Moreover, it is not possible to mention the effect of aluminum, iron oxide and zinc additives on tribology performance in serum and SBF media.

Optical microscopy images of worn surface of Al containing coatings in different testing environment are given in Figure 4.17.

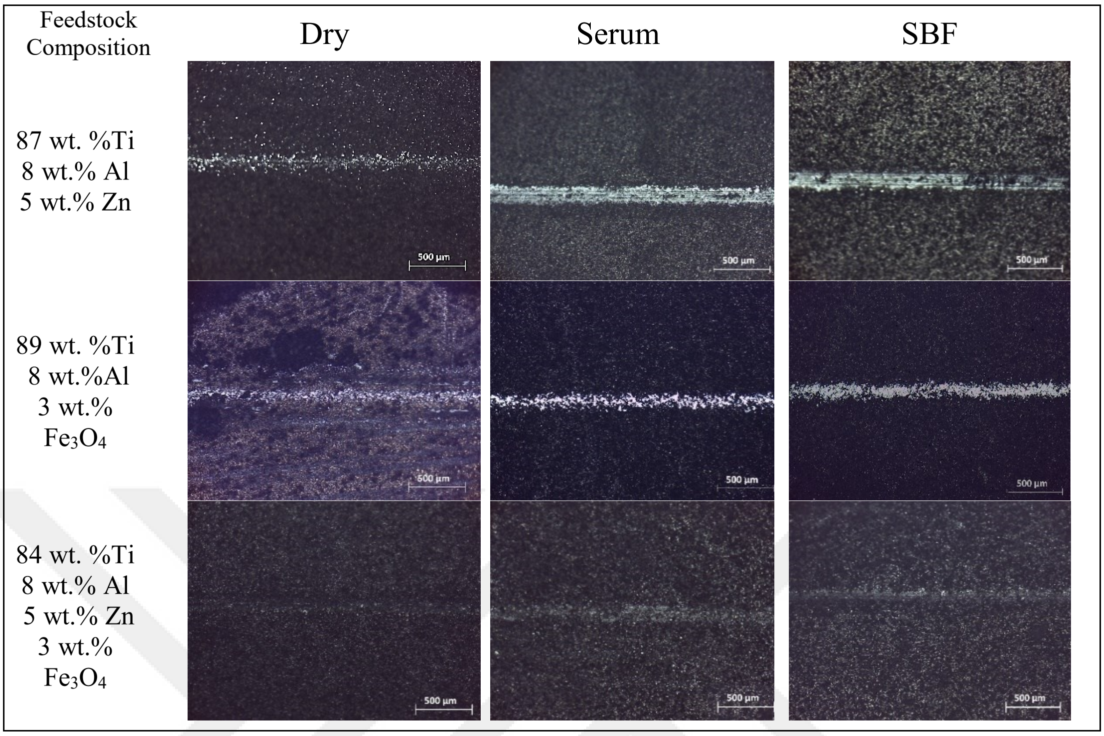

Figure 4.17: OM images of worn surfaces of Al containing coatings after thermal oxidation

Only around 100 µm width wear track observed on the worn surface of Al containing coating in serum and SBF environment. In contrary to Co-Cr substrate, in dry sliding conditions, it is difficult to observe wear track due to lubricant effect of ceramic-ceramic interaction during wear test. Worn surfaces of Al containing coatings were scanned with profilometer but unfortunately, no rational result could be determined. Moreover, in dry sliding conditions for surface of counter bodies are clean and just the wear scratches can be seen. These observations may thought the abrasive wear mechanism is dominant during dry sliding condition (Figure 4.18). Additionally for Zn containing coatings, smaller deformation marks were detected from the surface of alumina ball, which is parallel with the comments of previous results (friction coefficients.

It was understood from these observations, even under extreme contact pressure (around 840 MPa) during wear test in any environment only trimming of rough surfaces is possible for oxidized coating which is favorable indeed for biomedical implants working under high wear conditions especially for hip or knee joint implants.

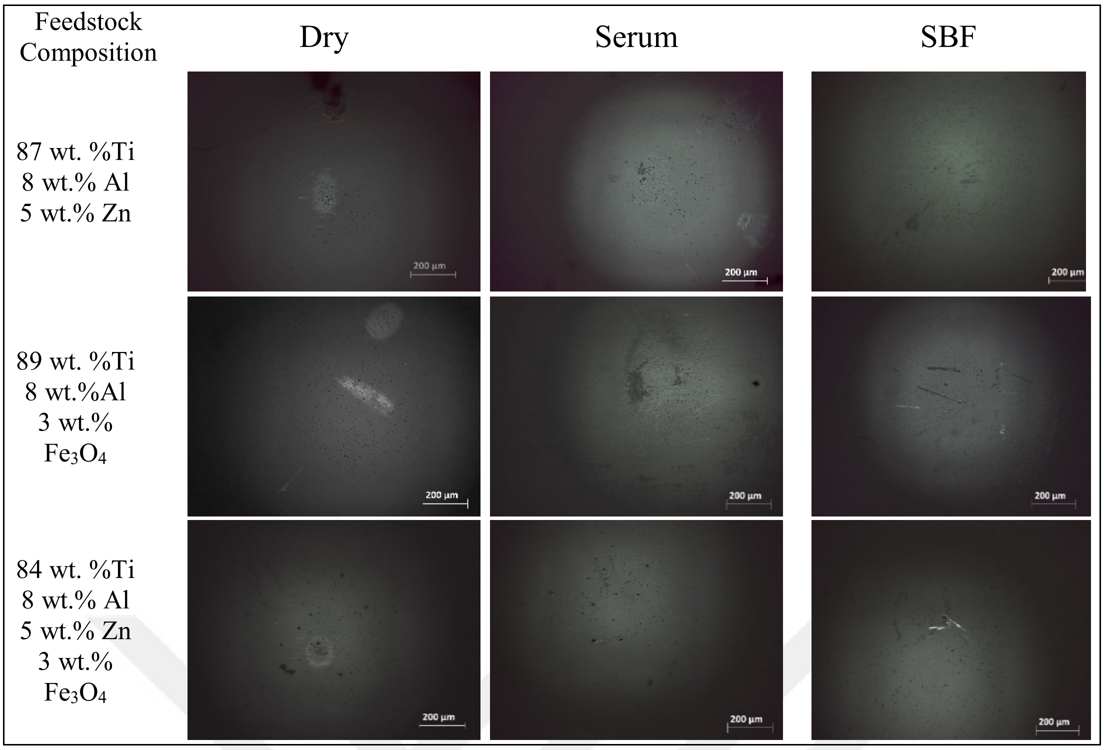

Figure 4.18: Wear scar appereance of alumina ball for the Al containing coatings after thermal oxidation

4.6 Biological Test of Al Containing Coatings

In this section, result of the biological test for aluminum containing coatings will be explained briefly.

4.6.1 In vitro bioactivity test

SEM images of the surfaces after immersion in SBF for 1 week and 4 weeks at 36.5 ºC are given in Figure 4.19. Like as copper containing coatings, the surface of aluminum containing coating, showed the formation of a new structure in the same morphology with Hydroxyapatite after 4 weeks [8]. However, after 1 week of immersion it is not possible to mention about any appearances on the surfaces. This result may be explain with differences in electro negativity of copper, titanium, aluminum and zinc. It is weel known from the literature that, Hydroxyapatite like structures formed as a result of electron change between media and the surfaces. Therefore, electoronegativity of copper may lead early formations than others.

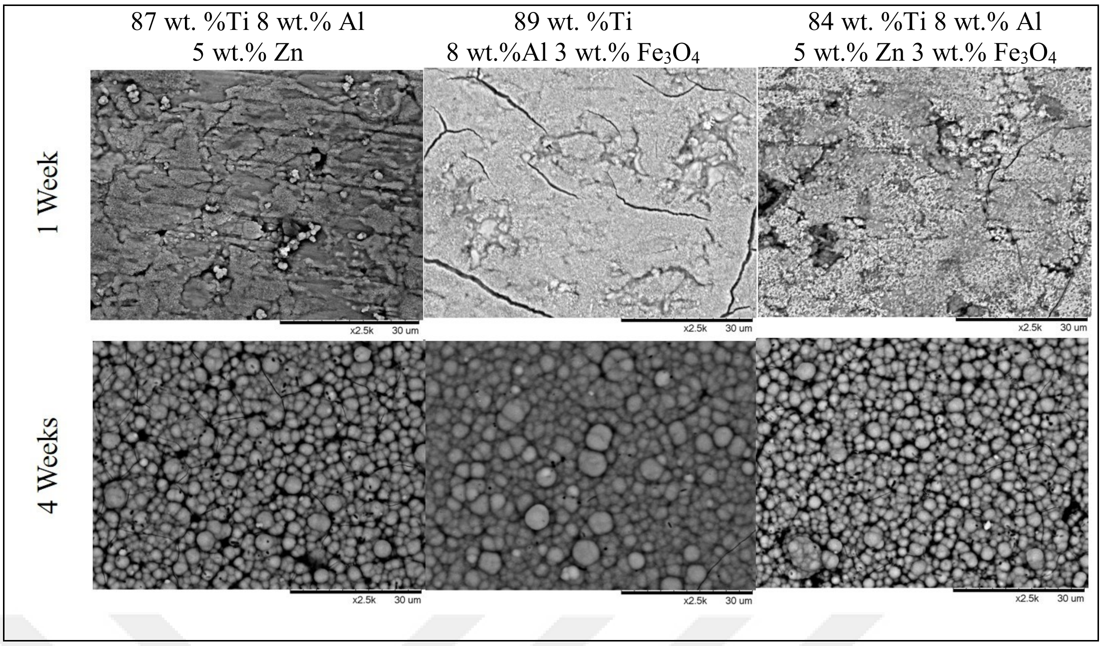

Figure 4.19: SEM micrographs of the Al containing coatings after 1 and 4 weeks in vitro bioactivity test

5. CONCLUSION

In recent master thesis study as part of research project supported by TUBITAK (Project No: 214M246), surface of ASTM F75 grade cobalt-chromium alloy was modified by the sequential application of cold gas dynamic spray and thermal oxidation processes (for 60 hour at 600 ºC). Based on experimental studies including structural characterization, mechanical properties and biological tests results obtained from this study can be summarized as;

- Copper and aluminum additives increase the efficiency of cold gas dynamic spray process and around 450 µm thick coatings were produced without any discontinuity on interface between substrate and coating, any unfavorable defect, with well distribution of additives. Moreover, zinc and iron oxide additives did not affect the efficiency of coating process.
- After thermal oxidation around 2-3 µm thick stable oxide layer formed on the outermost surface. But unfortunately, because of high mechanical effect during metallographic processes discontinuities and cracks were observed in OM and SEM observations.
- When the copper content decrease in the feedstock, coatings started to exhibit discontinuities and high porosities. In that respect further characterizations were performed just for coating deposited by feedstock 5 wt. % Cu-3 wt.% Fe_3O_4- 92 wt.% Ti.
- During thermal oxidation high diffusion of oxygen throughout the cross-section of coating was observed in EDX area and line scan analyses for all compositions.
- EDX area and line scan analyses of copper containing coating showed that, during thermal oxidation, copper preserve the metallic form or in the other word titanium particles did not let the oxidation of copper particles because of having higher affinity to oxygen and in microstructural examinations titanium-oxygen solid solution regions were detected around all copper particles.
- From the SEM examinations, for Zn containing coatings, zinc-titanium intermetallic compounds, for Al containing coatings aluminum-titanium intermetallic compounds were detected beside titanium solid solution phases.

- For all the coatings which contain iron oxide, particle boundaries were established as settlement places for iron oxide particles due to possible fragmentations during deposition of feedstock.
- XRD analyses before thermal oxidation showed that no chemical reaction took place during cold spray process and only peaks of feedstock composition were determined. In the other respect, after thermal oxidation oxide layer on the outermost surface consist of mainly titanium oxide in the form of rutile and small amount of other additives.
- For all the cases surface roughness was increased around 5-6 times due to natural outcome of oxidation of titanium. This result provide high bioactivity to the coatings.
- Cross-sectional and surface hardness measurements showed that, after thermal oxidation coatings reach around 450 $HV_{0.025}$ and 900 HV respectively.
- Tribological test results revealed that, all the coatings showed higher wear resistance than cobalt-chromium substrate in dry, serum and SBF media. Even in the serum and SBF environment high friction coefficients were observed for the coatings due to chemical reaction on the surface and extreme contact pressures, no rational result could obtain from 2D profiles of worn surfaces. Additionally, zinc containing coatings exhibit super low friction coefficient in dry media due to possible lubricant effect of metallic zinc and/or zinc-titanium intermetallic compound.
- Lastly, according to in vitro bioactivity tests titanium based multilayer coatings show promising results for further biomedical applications.

Briefly stated, titanium based coatings can be produced on the surface of ASTM F75 grade cobalt-chromium alloy by the sequential application of cold gas dynamic spray and thermal oxidation processes with higher hardness and wear resistance and possible higher bioactivity. Additionally, copper or zinc additions in to titanium may bring antibacterial behavior. Moreover, iron oxide particles in magnetite form may enlarge the application area of coatings.

REFERENCES

[1] **Jacobs, J.J., Skipor, A.K., Doom, P.F., Campbell, P., Schmalzried, T.P., Black, J., and Amstutz, H.C.** (1996). Cobalt and chromium concentrations in patients with metal on metal total hip replacements, *Clinical Orthopaedics and Related Research*, 329 SUPPL.),(256-263).

[2] **Martínez, R., Escobedo, J.C., Cortés, D.A., Alves, G.G., Linhares, A.B.R., Granjeiro, J.M., Prado, M., Ortiz, J.C., Almanza, J.M., and Múzquiz-Ramos, E.M.** (2013). In vitro bioactivity and biocompatibility of a Co–Cr–Mo alloy after heat treatment in contact with different bioactive systems, *Ceramics International*, 39(2),(2003-2011).

[3] **Marti, A.** (2000). Cobalt-base alloys used in bone surgery, *Injury Injury*, 31(5),(18-21).

[4] **Oksiuta, Z., Dabrowski, J.R., and Olszyna, A.** (2009). Co–Cr–Mo-based composite reinforced with bioactive glass, *Journal of Materials Processing Technology*, 209(2),(978-985).

[5] **Gomez, M., Mancha, H., Salinas, A., Rodriguez, J.L., Escobedo, J., Castro, M., and Mendez, M.** (1997). Relationship between microstructure and ductility of investment cast ASTM F-75 implant alloy, *Journal of Biomedical Materials Research*, 34(2),(157-163).

[6] **Kamachimudali, U., Sridhar, T.M., and Raj, B.** (2003). Corrosion of bio implants, *Sadhana Sadhana*, 28(3-4),(601-637).

[7] **Guleryuz, H. and Cimenoglu, H.** (2004). Effect of thermal oxidation on corrosion and corrosion-wear behaviour of a Ti-6A1-4V alloy, *Biomaterials*, 25(16),(3325-3333).

[8] **Çetiner., D.,** (2015), Biyomedikal Uygulamalar İçin Astm F75 Kobalt-Krom Alaşiminin Yüzey Modifikasyonu, Master Thesis, MSc, Materials Science and Engineering Department, Istanbul Technical University, Istanbul.

[9] **Bloyce, A., Qi, P.Y., Dong, H., and Bell, T.** (1998). Surface modification of titanium alloys for combined improvements in corrosion and wear resistance, *Surface and Coatings Technology*, 107(2–3),(125-132).

[10] **Dong, H. and Bell, T.** (1999). Tribological behaviour of alumina sliding against Ti6Al4V in unlubricated contact, *Wear*, 225–229, Part 2(874-884).

[11] **Davis, J.R. and International, A.**,(2003) Handbook of Materials for Medical Devices.(ASM International.

[12] **Ratner, B.D., Hoffman, A.S., Schoen, F.J., and Lemons, J.E.**,(2014) Biomaterials Science : an Introduction to Materials in Medicine. Saint Louis: Elsevier Science.

[13] **Niinomi, M., Narushima, T., and Nakai, M.**,(2015) Advances in Metallic Biomaterials : Processing and Applications. Springer Series in Biomaterials Science and Engineering;4. Berlin, Heidelberg: Springer Berlin Heidelberg.

[14] **Park, J.B.**,(2003) Biomaterials : principles and applications. Boca Raton: CRC Press.

[15] **Pilliar, R.M.**, (2009) Metallic Biomaterials, in Biomedical Materials, Narayan, Editor. Springer US: Boston, MA. (41-81).

[16] **Paulus, A., Ebinger, K., Hasselt, S., Jansson, V., Bader, R., Kretzer, J.P., and Utzschneider, S.** (2017). Biologic Effects Of Metal Wear Particles And Ions, *Bone & Joint Journal Orthopaedic Proceedings Supplement*, 99-B(SUPP 5),(80-80).

[17] **Chen, G. and Xu, W.D.** (2008). Biological effects of metal on metal hip prostheses, *J. Clin. Rehab. Tissue Eng. Res. Journal of Clinical Rehabilitative Tissue Engineering Research*, 12(9),(1729-1732).

[18] **Okazaki, Y. and Gotoh, E.** (2008). Metal release from stainless steel, Co-Cr-Mo-Ni-Fe and Ni-Ti alloys in vascular implants, *Corros. Sci. Corrosion Science*, 50(12),(3429-3438).

[19] **Hallab, N.J. and Jacobs, J.J.** (2009). Biologic Effects of Implant Debris, *Bulletin /*, 67(2),(182-188).

[20] **Yaszemski, M.J., Trantolo, D.J., Lewandrowski, K.-U., Hasirci, V., Altobelli, D.E., and Wise, D.L.** (2004). Biomaterials in Orthopedics, CRC Press.

[21] **Sharma, R.K. and Agrawal, M.** (2005). Biological effects of heavy metals: An overview, *Journal of environmental biology* , 26(2),(301-314).

[22] **Elias, C.N., Lima, J.H.C., Valiev, R., and Meyers, M.A.** (2008). Biomedical applications of titanium and its alloys, *JOM*, 60(3),(46-49).

[23] **Niinomi, M., Liu, Y., Nakai, M., Liu, H., and Li, H.** (2016). Biomedical titanium alloys with Young's moduli close to that of cortical bone, *Regen Biomater*, 3(3),(173-185).

[24] **Geetha, M., Singh, A.K., Asokamani, R., and Gogia, A.K.** (2009). Ti based biomaterials, the ultimate choice for orthopaedic implants – A review, *Progress in Materials Science*, 54(3),(397-425).

[25] **Disegi, J.A., Kennedy, R.L., and Pilliar, R.**,(1999) Cobalt-base Alloys for Biomedical Applications, ASTM International.

[26] **Taylor, R.N.J. and Waterhouse, R.B.** (1983). A study of the ageing behaviour of a cobalt based implant alloy, *Journal of Materials Science*, 18(11),(3265-3280).

[27] **Park, J.B. and Bronzino, J.D.**,(2002) Biomaterials: Principles and Applications, CRC Press.

[28] **Patel, B., Favaro, G., Inam, F., Reece, M.J., Angadji, A., Bonfield, W., Huang, J., and Edirisinghe, M.** (2012). Cobalt-based orthopaedic alloys: Relationship between forming route, microstructure and

tribological performance, *Materials Science and Engineering: C*, 32(5),(1222-1229).

[29] **Davis, J.R., International, A.S.M., and Handbook, C.**,(2000) ASM specialty handbook : nickel, cobalt, and their alloys. Materials Park, OH: ASM International.

[30] **Narayan, R.**,(2009) Biomedical materials. Narayan, Editor. Springer US: Boston, MA.

[31] **Park, J.B. and Lakes, R.S.**,(2010) Biomaterials : an introduction. New York, NY: Springer.

[32] **Gopi, D., Ramya, S., Rajeswari, D., and Kavitha, L.** (2013). Corrosion protection performance of porous strontium hydroxyapatite coating on polypyrrole coated 316L stainless steel, *Colloids and surfaces. B, Biointerfaces*, 107(130-136).

[33] **Anne Pauline, S., Kamachi Mudali, U., and Rajendran, N.** (2013). Fabrication of nanoporous Sr incorporated TiO2 coating on 316L SS: Evaluation of bioactivity and corrosion protection, *Materials Chemistry and Physics Materials Chemistry and Physics*, 142(1),(27-36).

[34] **Sutha, S., Karunakaran, G., and Rajendran, V.** (2013). Enhancement of antimicrobial and long-term biostability of the zinc-incorporated hydroxyapatite coated 316L stainless steel implant for biomedical application, *Ceramics International*, 39(5),(5205-5212).

[35] **Arslan, E., Totik, Y., Demirci, E.E., Vangolu, Y., Alsaran, A., and Efeoglu, I.** (2009). High temperature wear behavior of aluminum oxide layers produced by AC micro arc oxidation, *Surface and Coatings Technology*, 204(6-7),(829-833).

[36] **Krzakala, A., Kazek-Kesik, A., and Simka, W.** (2013). Application of plasma electrolytic oxidation to bioactive surface formation on titanium and its alloys, *RSC Adv. RSC Advances*, 3(43),(19725-19743).

[37] **Nguyen, H.** (2004). The effect of sol–gel-formed calcium phosphate coatings on bone ingrowth and osteoconductivity of porous-surfaced Ti alloy implants, *Biomaterials*, 25(5),(865-876).

[38] **Harman, M.K., Banks, S.A., and Andrew Hodge, W.** (1997). Wear analysis of a retrieved hip implant with titanium nitride coating, *Journal of Arthroplasty*, 12(8),(938-945).

[39] **Papyrin, A.**,(2007) Cold spray technology. Amsterdam; London; Paris: Elsevier.

[40] **Champagne, V.K.**,(2007) The cold spray materials deposition process : fundamentals and applications. Cambridge: Woodhead.

[41] **Papyrin, A.N.**, (2002) Cold Spray Process for Cost-Sensitive Applications, in High Performance Metallic Materials for Cost Sensitive Applications. John Wiley & Sons, Inc. (137-149).

[42] **Li, W.-Y., Liao, H., Douchy, G., and Coddet, C.** (2007). Optimal design of a cold spray nozzle by numerical analysis of particle velocity and

experimental validation with 316L stainless steel powder, *Materials & Design*, 28(7),(2129-2137).

[43] **Assadi, H., Gärtner, F., Stoltenhoff, T., and Kreye, H.** (2003). Bonding mechanism in cold gas spraying, *Acta Materialia Acta Materialia*, 51(15),(4379-4394).

[44] **Papyrin, A.** (2001). Cold Spray Technology - One of the developers of this high-interest coating process explains how it works and describes its advantages over conventional thermal spray methods, *Advanced materials & processes.*, 159(9),(49).

[45] **Klinkov, S.V., Kosarev, V.F., and Rein, M.** (2005). Cold spray deposition: Significance of particle impact phenomena, *Aerospace Science and Technology*, 9(7),(582-591).

[46] **Fauchais, P.**, (2015) - Current status and future directions of thermal spray coatings and techniques - Edt. Espallargas, Nuria, in Future Development of Thermal Spray Coatings. Woodhead Publishing (17-49).

[47] **Van Steenkiste, T.H., Smith, J.R., and Teets, R.E.** (2002). Aluminum coatings via kinetic spray with relatively large powder particles, *Surface and Coatings Technology*, 154(2–3),(237-252).

[48] **Fukumoto, M., Wada, H., Tanabe, K., Yamada, M., Yamaguchi, E., Niwa, A., Sugimoto, M., and Izawa, M.** (2007). Effect of Substrate Temperature on Deposition Behavior of Copper Particles on Substrate Surfaces in the Cold Spray Process, *Journal Of Thermal Spray Technology*, 16(5-6),(643-650).

[49] **King, P.C., Zahiri, S.H., and Jahedi, M.Z.** (2008). Rare earth/metal composite formation by cold spray, *Journal of Thermal Spray Technology*, 17(2),(221-227).

[50] **Raletz, F., Vardelle, M., and Ezo'o, G.** (2006). Critical particle velocity under cold spray conditions, *Surface and Coatings Technology*, 201(5),(1942-1947).

[51] **Zhou, X. and Mohanty, P.** (2012). Electrochemical behavior of cold sprayed hydroxyapatite/titanium composite in Hanks' solution, *Electrochimica Acta*, 65(134-140).

[52] **Sun, J., Han, Y., and Cui, K.** (2008). Innovative fabrication of porous titanium coating on titanium by cold spraying and vacuum sintering, *Materials Letters*, 62(21-22),(3623-3625).

[53] **Bou-Saleh, Z., Shahryari, A., and Omanovic, S.** (2007). Enhancement of corrosion resistance of a biomedical grade 316LVM stainless steel by potentiodynamic cyclic polarization, *Thin Solid Films*, 515(11),(4727-4737).

[54] **Effah, E.A.B., Bianco, P.D., and Ducheyne, P.** (1995). Crystal structure of the surface oxide layer on titanium and its changes arising from immersion, *Journal of Biomedical Materials Research*, 29(1),(73-80).

[55] **Wen, M., Wen, C., Hodgson, P., and Li, Y.** (2012). Thermal oxidation behaviour of bulk titanium with nanocrystalline surface layer, *Corrosion Science*, 59(352-359).

[56] **Jamesh, M., Sankara Narayanan, T.S.N., and Chu, P.K.** (2013). Thermal oxidation of titanium: Evaluation of corrosion resistance as a function of cooling rate, *Materials Chemistry and Physics*, 138(2–3),(565-572).

[57] **Leyens, C. and Peters, M.** (2006). Titanium and Titanium Alloys : Fundamentals and Applications.

[58] **Diebold, U.** (2003). The surface science of titanium dioxide, *Surface Science Reports*, 48(5–8),(53-229).

[59] **Ashton, S.J. and Chambers, L.H.**, (1970) The Influence Of Microstructure On The Mechanical Properties Of Forged Alpha/Beta Titanium Alloys in The Science, Technology and Application of Titanium, Promisel, Editor. Pergamon. (879-889).

[60] **López, M.F., Jiménez, J.A., and Gutiérrez, A.** (2003). Corrosion study of surface-modified vanadium-free titanium alloys, *Electrochimica Acta*, 48(10),(1395-1401).

[61] **Wiklund, U. and Hutchings, I.M.** (2001). Investigation of surface treatments for galling protection of titanium alloys, *Wear*, 251(1–12),(1034-1041).

[62] **Komotori, J., Lee, B.J., Dong, H., and Dearnley, P.A.** (2001). Corrosion response of surface engineered titanium alloys damaged by prior abrasion, *Wear*, 251(1–12),(1239-1249).

[63] **Qi, P.Y., Li, X.Y., Dong, H., and Bell, T.** (2002). Characterisation of the palladium-modified thermal oxidation-treated titanium, *Materials Science and Engineering: A*, 326(2),(330-342).

[64] **Wang, X.-X., Yan, W., Hayakawa, S., Tsuru, K., and Osaka, A.** (2003). Apatite deposition on thermally and anodically oxidized titanium surfaces in a simulated body fluid, *Biomaterials*, 24(25),(4631-4637).

[65] **García-Alonso, M.C., Saldaña, L., Vallés, G., González-Carrasco, J.L., González-Cabrero, J., Martínez, M.E., Gil-Garay, E., and Munuera, L.** (2003). In vitro corrosion behaviour and osteoblast response of thermally oxidised Ti6Al4V alloy, *Biomaterials*, 24(1),(19-26).

[66] **Cimenoglu, H., Meydanoglu, O., Baydogan, M., Bermek, H., Huner, P., and Kayali, E.S.** (2011). Characterization of thermally oxidized Ti6Al7Nb alloy for biological applications, *Metals and Materials International*, 17(5),(765-770).

[67] **Mani, G., Feldman, M.D., Oh, S., and Agrawal, C.M.** (2009). Surface modification of cobalt–chromium–tungsten–nickel alloy using octadecyltrichlorosilanes, *Applied Surface Science*, 255(11),(5961-5970).

[68] **Onate, J.J., Comin, M., Braceras, J., Garcia, A., Viviente, J.L., Brizuela, M., Garagorri, N., Peris, J.L., and Alava, J.I.** (2011). Wear reduction effect on ultra-high-molecular-weight polyethylene by application of hard coatings and ion implantation on cobalt chromium alloy, as

measured in a knee wear simulation machine, *Surface and Coatings Technology*, 142, (1056-1062).

[69] **Wei, R., Booker, T., Rincon, C., and Arps, J.** (2004). High-intensity plasma ion nitriding of orthopedic materials, *Surface And Coatings Technology.*, 186(1-2),(305-313).

[70] **Cüneyt Tas, A.** (2000). Synthesis of biomimetic Ca-hydroxyapatite powders at 37°C in synthetic body fluids, *Biomaterials*, 21(14), (1429-1438).

[71] **Alves, V.A., Reis, R.Q., Santos, I.C.B., Souza, D.G., de F. Gonçalves, T., Pereira-da-Silva, M.A., Rossi, A., and da Silva, L.A.** (2009). In situ impedance spectroscopy study of the electrochemical corrosion of Ti and Ti6Al4V in simulated body fluid at 25°C and 37°C, *Corrosion Science Corrosion Science*, 51(10), (2473-2482).

[72] **Wang, Z., Huang, W., and Ma, Y.** (2014). Micro-scale abrasive wear behavior of medical implant material Ti-25Nb-3Mo-3Zr-2Sn alloy on various friction pairs, *MSC Materials Science & Engineering C*, 42, (211-218).

APPENDICES

APPENDIX A: Friction coefficient curves of substrate and oxidized coatings

APPENDIX A: Friction coefficient curves of substrate and oxidized coatings

Feedstock Composition	
Substrate	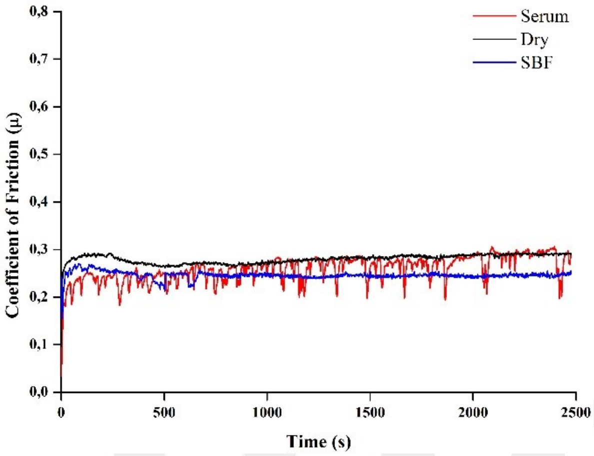
92 wt. % Ti 5 wt.% Cu 3 wt.% Fe_3O_4	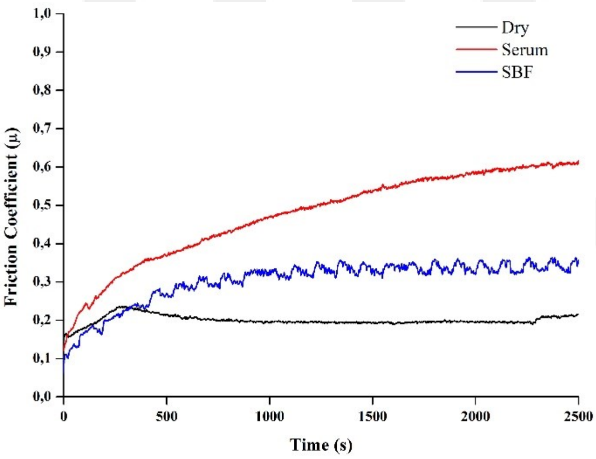
87 wt. %Ti 8 wt.%Al 5 wt.% Zn	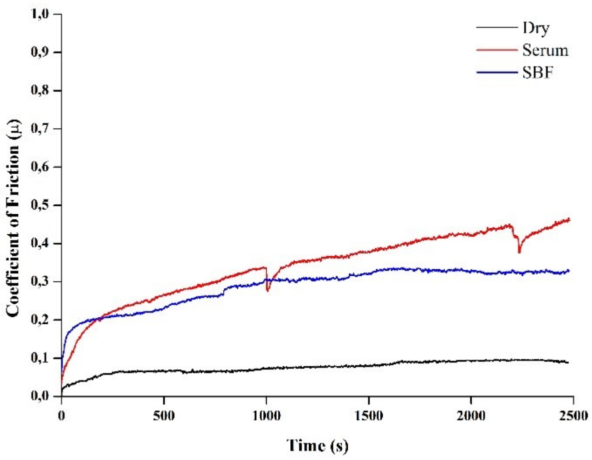

Figure A. 1: Friction coefficient curves of susbtrate and oxidized coatings

89 wt. %Ti

8 wt.%Al

3 wt.% Fe_3O_4

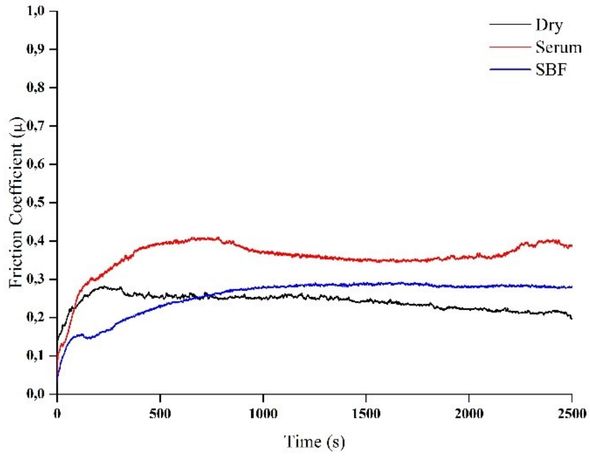

84 wt. %Ti

8 wt.%Al

5 wt. % Zn

3 wt.% Fe_3O_4

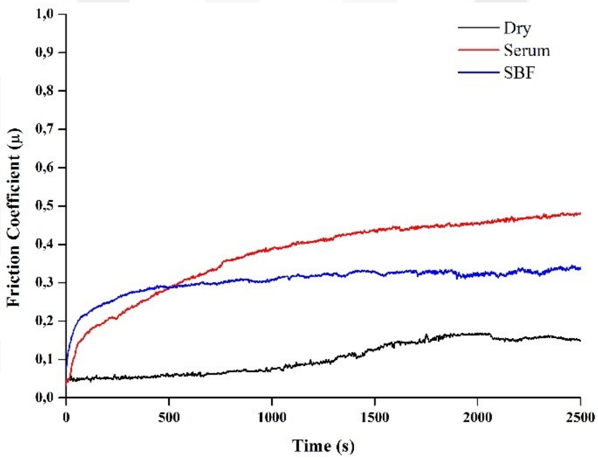

Figure A. 1 (Cont.): Friction coefficient curves of susbtrate and oxidized coatings

CURRICULUM VITAE

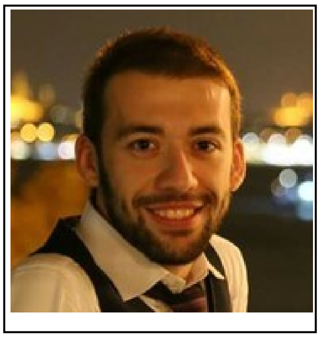

Name Surname : **Ahmet Hilmi PAKSOY**

Place and Date of Birth : **NEVŞEHİR / 15/06/1991**

E-Mail : **paksoyah@itu.edu.tr**

EDUCATION :

- **B.Sc.** : 2014, Ege University, Engineering Faculty, Mechanical Engineering Department

PUBLICATIONS, PRESENTATIONS AND PATENTS ON THE THESIS:

- Thermal oxidation of cold sprayed Ti-Cu-Fe_3O_4 coating. **AH Paksoy**, O Tazegul, D Cetiner, M Baydogan, E Atar, H Güleryüz, H Cımenoglu, SerbiaTrib'17- May 2017.

OTHER PUBLICATIONS, PRESENTATIONS AND PATENTS:

ARTICLES:

- Influence of laser surface melting on the characteristics of Stellite 12 plasma transferred arc hardfacing deposit. SAA Dilawary, A Motallebzadeh, **AH Paksoy,** M Afzal, E Atar, H Cimenoglu, Surface Coating and Technology 317 (2017) 110–116.
- The Effect of Sic Reinforcement On Tribological Behaviour of Cold Sprayed Coatings In Water. O Deprem, **AH Paksoy**, O Tazegul, H Cimenoglu, Tribology - Materials, Surfaces & Interfaces 11-1 (2017) 14–18.
- Tribology of SiCp Reinforced Al-12Si Matrix Composite Coatings In Water. **AH Paksoy**, O Deprem, O Tazegul, H Cimenoglu Tribology International 110 (2017) 392–400.
- Formation Of Corrosion-Resistant Alumina Coating On 6061 Aluminum Alloy By The Combination Of Micro Arc Oxidation And Sealing Treatments. **AH**

Paksoy, F Muhaffel, M Koca, O Gokce, S Mohammadzadeh, H Cimenoglu. Materials and Technology, 51:1, (2017).

- Characteristic Of MAO Coatings Formed On $CuAl_2$ In-Situ Reinforced Aluminum Matrix Composites. DI Mafouz **AH Paksoy**, F Muhaffel, O Tazegul, H Cimenoglu. Archives of Material Science and Engineering 76:2, (2016) 60-63
- Structural Characterization of Thermally Oxidized Titanium Based Coating. D Cetiner, **AH Paksoy**, O Tazegul, E Atar, H Cimenoglu. Journal of Achievements in Materials and Manufacturing Engineering 75:2 (2016).

CONFERENCE PAPERS:

- Production Of A Coating Containing Ca, P and Zn on AZ31 Magnesium Alloy By Micro Arc Oxidation AP Santos, F Muhaffel, **AH Paksoy**, H Cimenoglu. International Scientific Conference UNITECH'16. November 2016
- Laser modification of the Stellite12 Hardfacing PTA Layer. SAA Dilawary, A Motallebzadeh, **AH Paksoy,** M Afzal, E Atar, H Cimenoglu. 16th International Materials Symposium IMSP'2016, October 2016
- Microstructural Investigation and Wear Performance Of Ductile Irons Treated By Two-Step Austempering Processes G Gider, Y Yurekturk, **AH Paksoy**, F Muhaffel, M Baydogan 16th International Materials Symposium IMSP'2016, October 2016.
- Influence Of Austempering Temperature On Microstructural And Mechanical Properties Of EN-GJS-500-7 And EN-GJS-600-3 Grades Nodular Cast Irons. G Gider, Y Yurekturk, **AH Paksoy**, F Muhaffel, M Baydogan. 5th Heat Treatment Symposium, June 2016.
- In Situ Production And Mechanical Properties Of Aluminum Matrix Aluminum Copper Intermetallic Composite DI Mafouz **AH Paksoy**, F Muhaffel, O Tazegul, H Cimenoglu. International Conference on Material Science and Technology April 2016.